
JVK
2004

Membrane Proteins

Mitochondria and respiratory chains

John F. Allen

School of Biological and Chemical Sciences,
Queen Mary, University of London

Queen Mary
University of London

Presentations
and
supplementary information

jfallen.org/lectures/

Queen Mary
University of London

Lectures in Membrane Proteins

References

- Nicholls DJ, Ferguson, SJ. Bioenergetics3. Academic Press/Elsevier Science 2002
- Molecular Biology of the Cell Bruce Alberts, Alexander Johnson, Julian Lewis, Martin Raff, Keith Roberts, and Peter Walter. 2002. Garland Science
- Lane N. Power, Sex, Suicide. Mitochondria and the Meaning of Life. Oxford University Press. October 2005

Specialist web sites

- Complex I Home Page
- News on the 3D structure from the Complex I Home Page
- Complex III Home Page
- Cytochrome oxidase home page. Complex IV, the subject of the lecture by Professor Peter Rich

Qo. The movie

- Qo.mov

Molecule of the Month

- ATP Synthase
- Bacteriorhodopsin
- Cytochrome c
- Cytochrome c Oxidase
- Photosystem I
- Photosystem II
- Potassium Channels

Relevant papers as pdf files. Please observe copyright

- Structure of the Hydrophilic Domain of Respiratory Complex I from Thermus thermophilus
- Structure of the Hydrophilic Domain of Respiratory Complex I from Thermus thermophilus pdf file
- An atypical haem in the cytochrome b6f complex pdf file
- Structure of the Cytochrome b6f Complex of Oxygenic Photosynthesis: Tuning the Cavity pdf file
- Protein synthesis by isolated pea mitochondria is dependent on the activity of respiratory complex II
- Structure for signalling and vectorial metabolism
- Energy transduction anchors genes in organelles
- The function of genomes in bioenergetic organelles
- Why do we still have a maternally inherited mitochondrial DNA? Insights from evolutionary medicine
- Power for life
- Chemiosmotic coupling: The Cost of Living Professor Peter Rich
- Power Games By Nick Lane
- Biodiversity: On the origin of bar codes By Nick Lane
- Photosynthesis - telling it like it is Review of Blankenship's Molecular Mechanisms of Photosynthesis

Nobel prizes

- 1978 Chemistry Nobel Prize to Peter Mitchell
- 1988 Chemistry Nobel Prize to Johann Deisenhofer, Robert Huber and Hartmut Michel
- 1997 Chemistry Nobel Prize to Paul D. Boyer, John E. Walker and Jens C. Skou

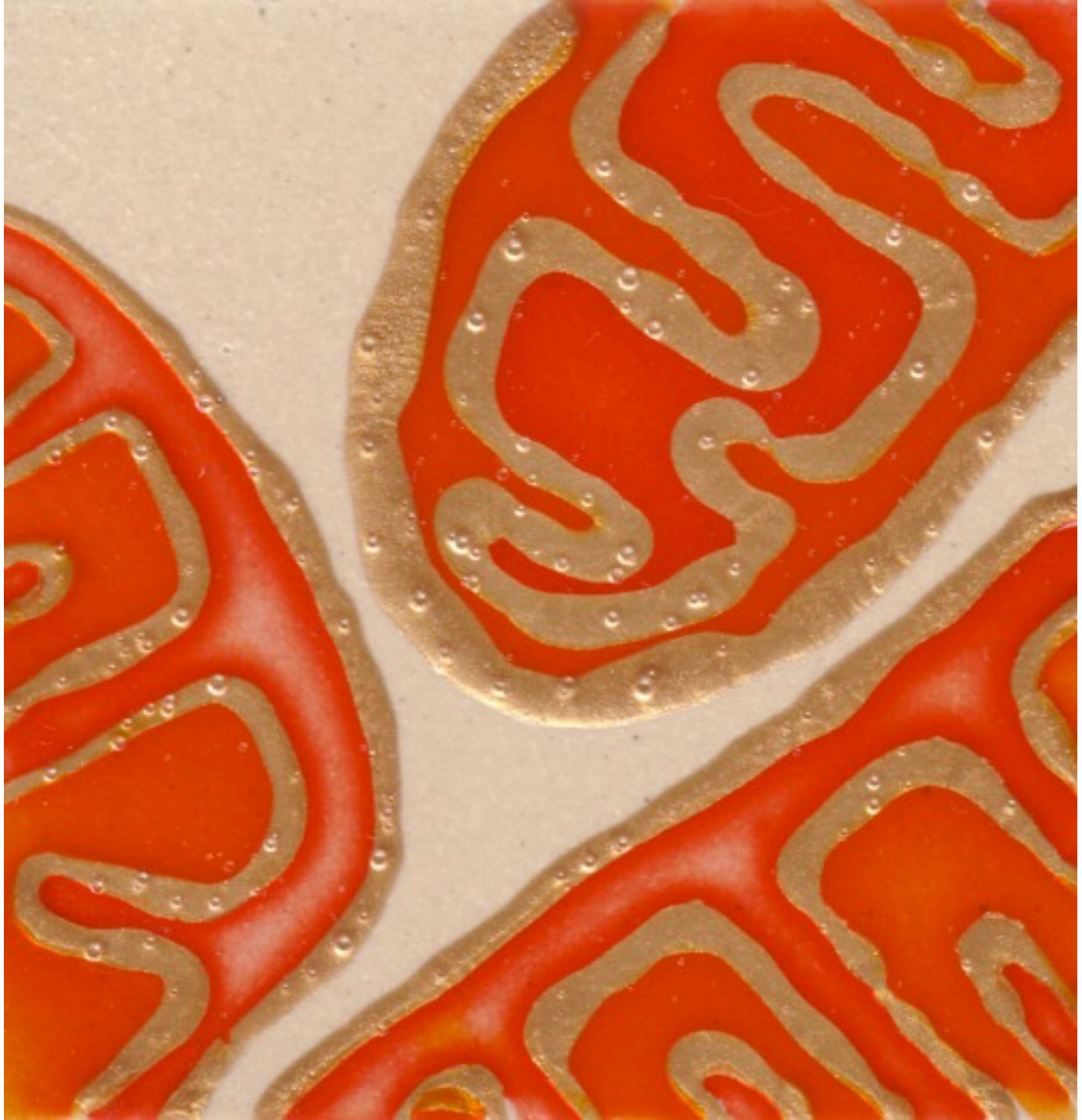

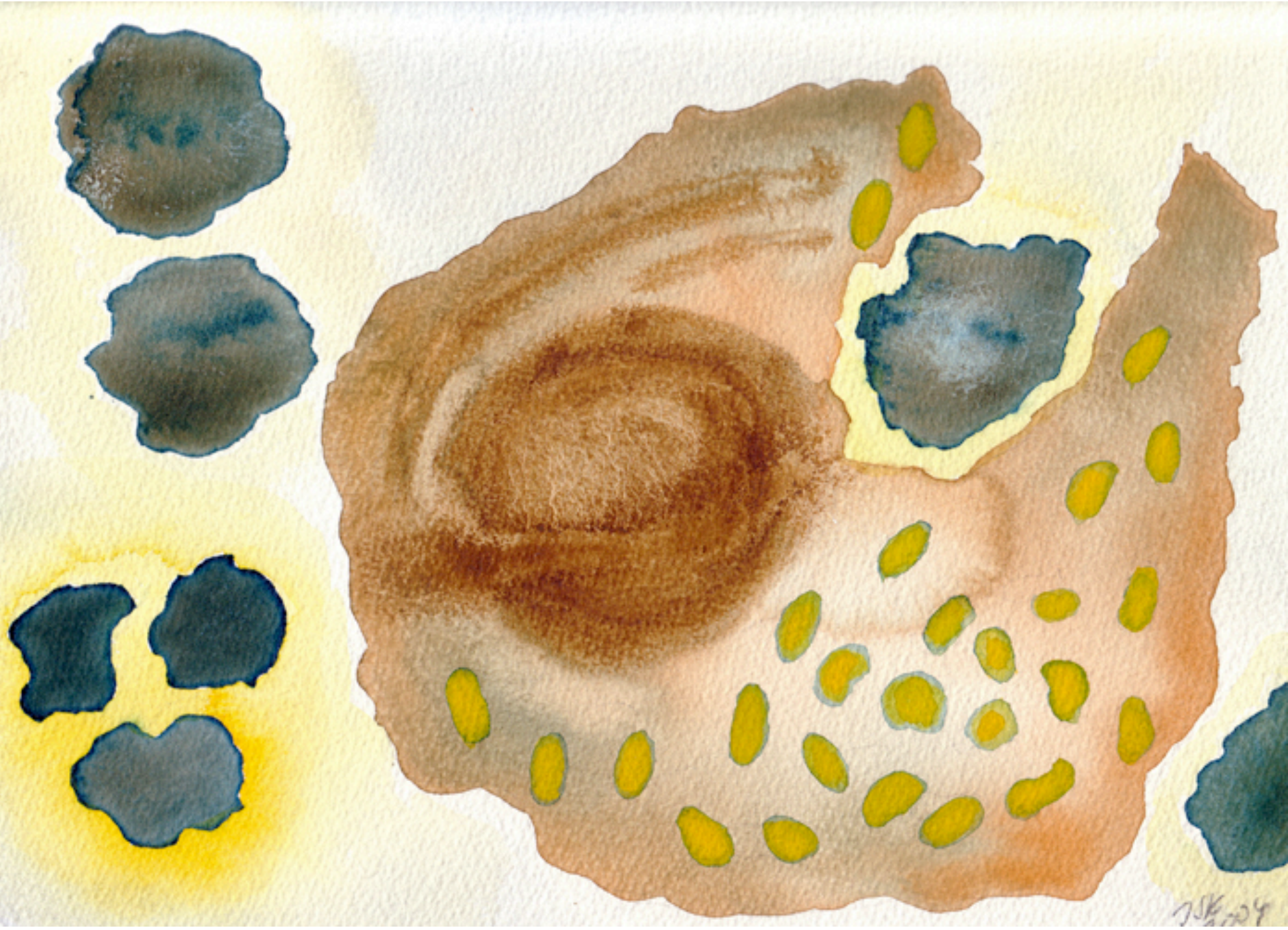

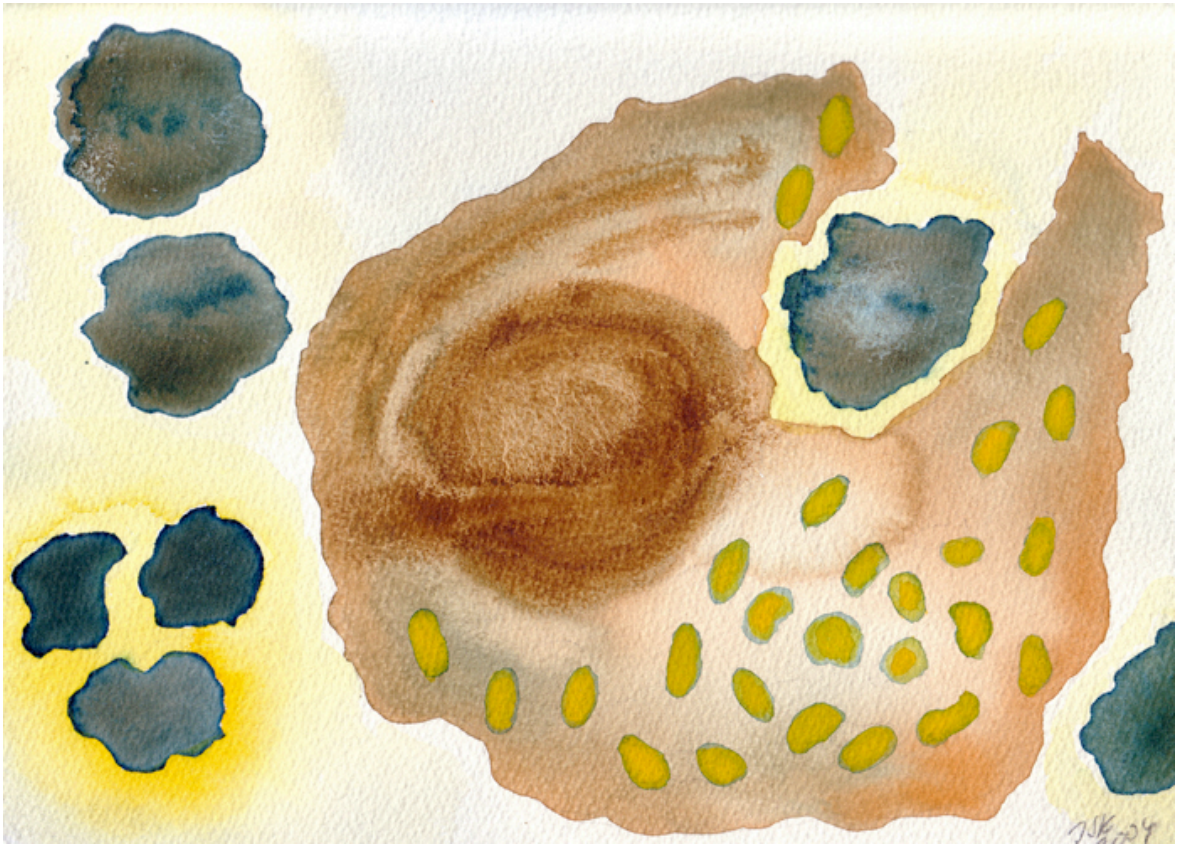

A large cell with things inside—in eukaryotes, energy generation is internalized in mitochondria

Bacteria ruled supreme on Earth for two billion years. They evolved almost unlimited biochemical versatility but never discovered the secrets of greater size or morphological complexity. Life on other planets may get stuck in the same rut. On Earth, large size and complexity only became possible once energy generation had been internalized in mitochondria. But why did bacteria never internalize their own energy generation? The answer lies in the tenacious survival of mitochondrial DNA, a two-billion-year-old paradox.

Complex I.

Structure and Function. Part 1.

jfallen.org/lectures/

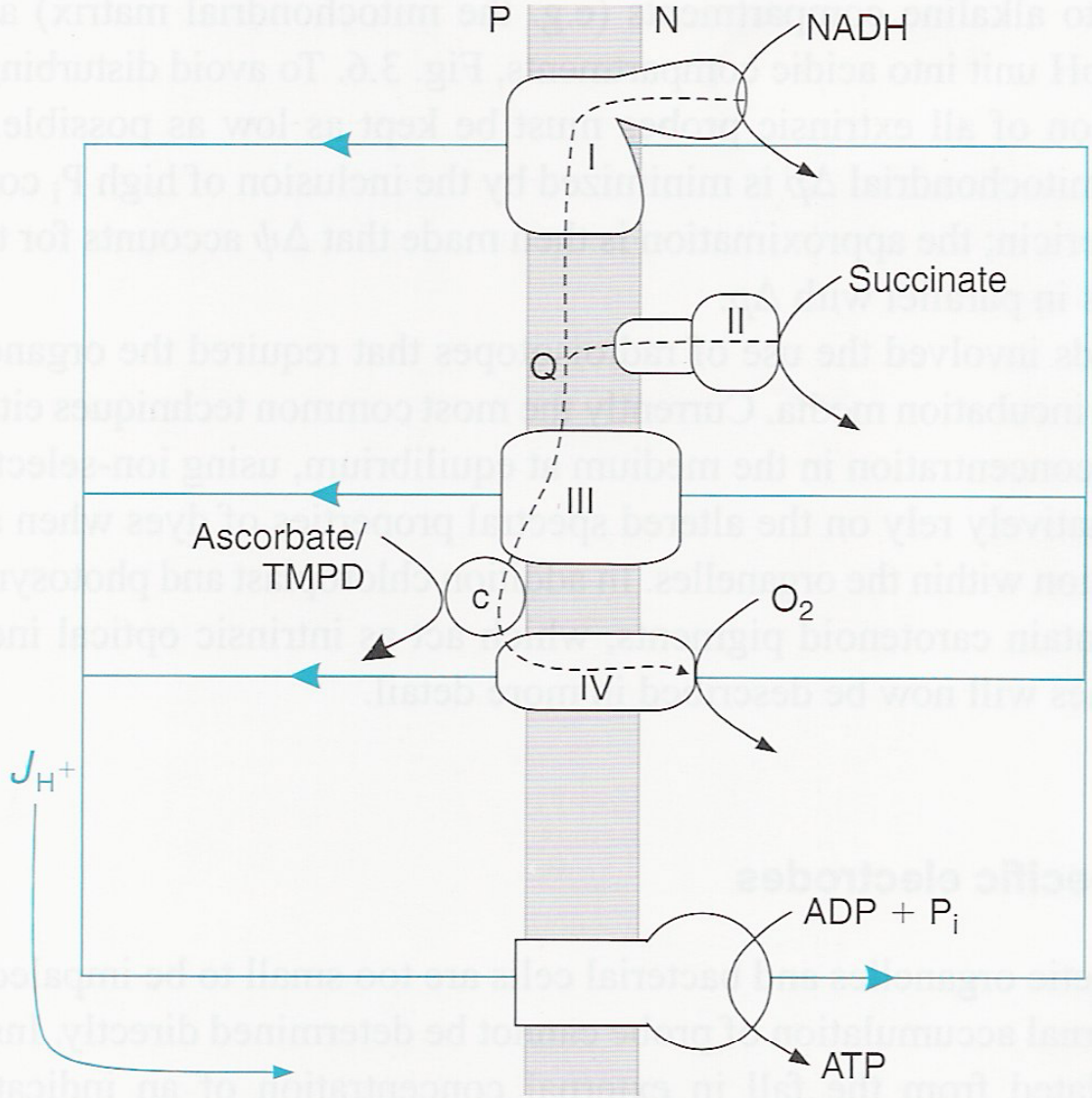

Figure 4.2 The mitochondrial respiratory chain consists of three proton pumps (complexes I, III and IV), which act in parallel with respect to the proton circuit and in series with respect to the electron flow.
Solid lines: pathway of proton flux; dotted line: pathway of electron transfer. For redox couples, see Table 3.2.

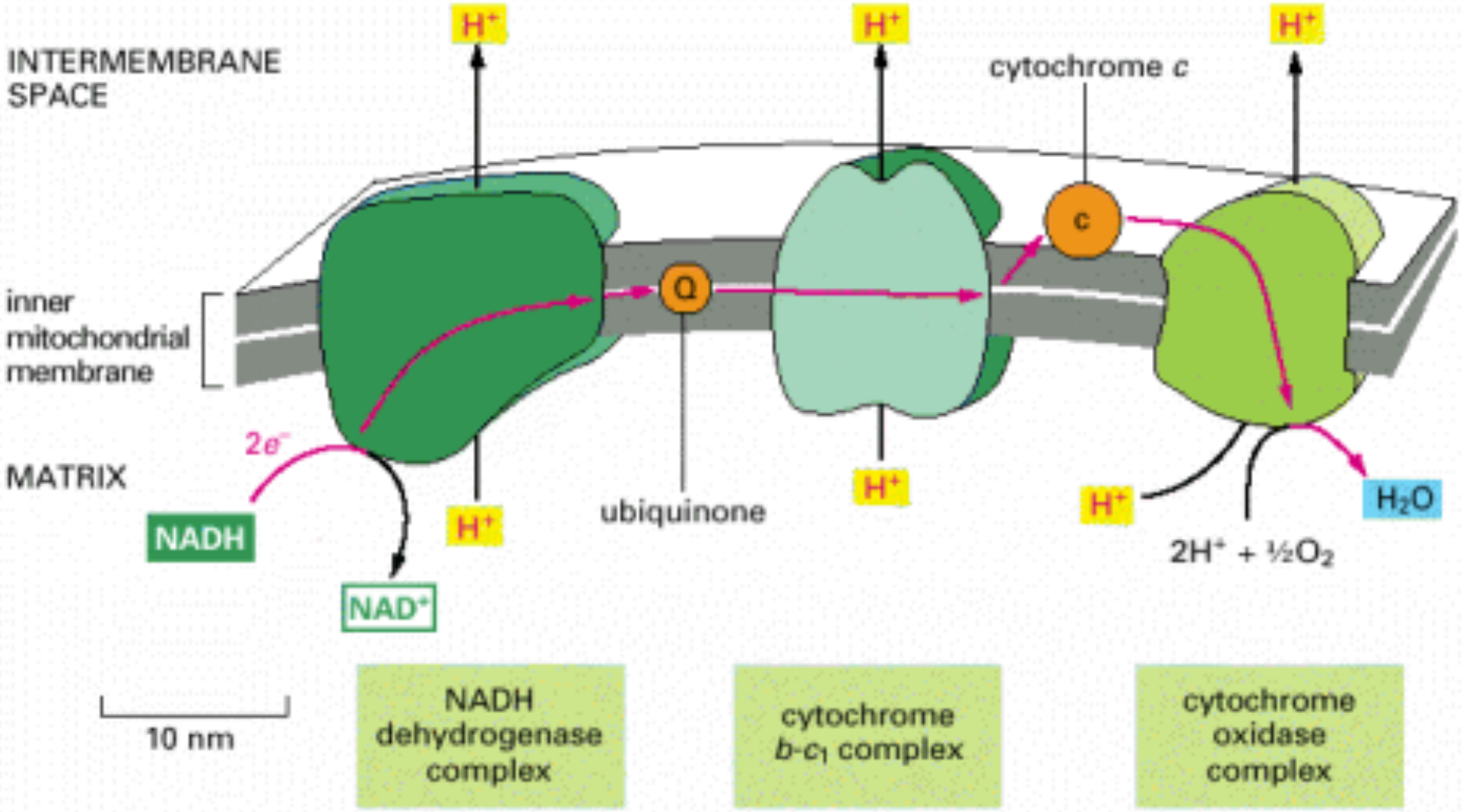

The Respiratory Chain Includes Three Large Enzyme Complexes Embedded in the Inner Membrane

Molecular Biology of the Cell Bruce Alberts, Alexander Johnson, Julian Lewis, Martin Raff, Keith Roberts, and Peter Walter. 2002

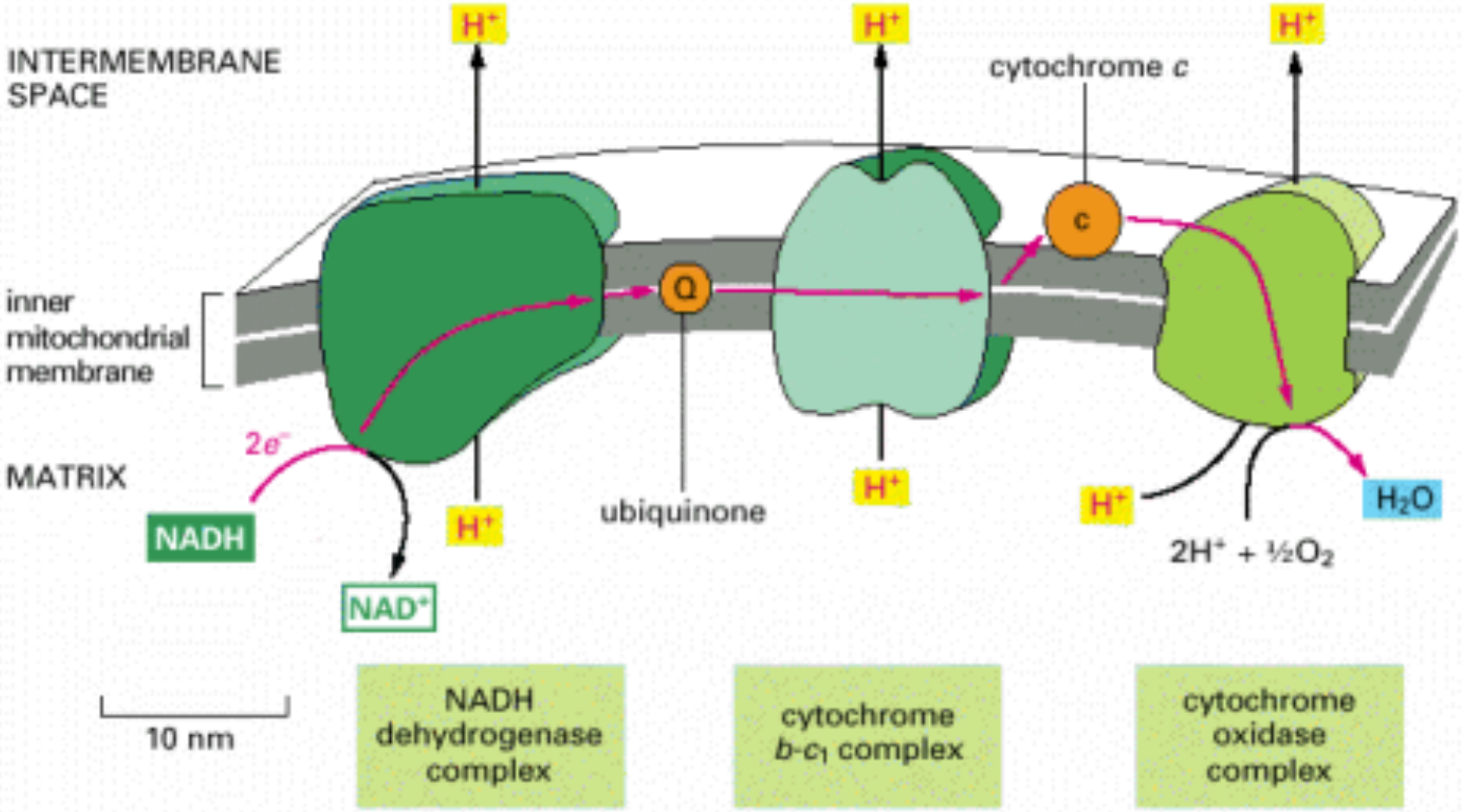

1. The NADH dehydrogenase complex (generally known as complex I) is the largest of the respiratory enzyme complexes, containing more than 40 polypeptide chains. It accepts electrons from NADH and passes them through a flavin and at least seven iron-sulfur centers to ubiquinone. Ubiquinone then transfers its electrons to a second respiratory enzyme complex, the cytochrome b-c_1 complex.

Molecular Biology of the Cell Bruce Alberts, Alexander Johnson, Julian Lewis, Martin Raff, Keith Roberts, and Peter Walter. 2002

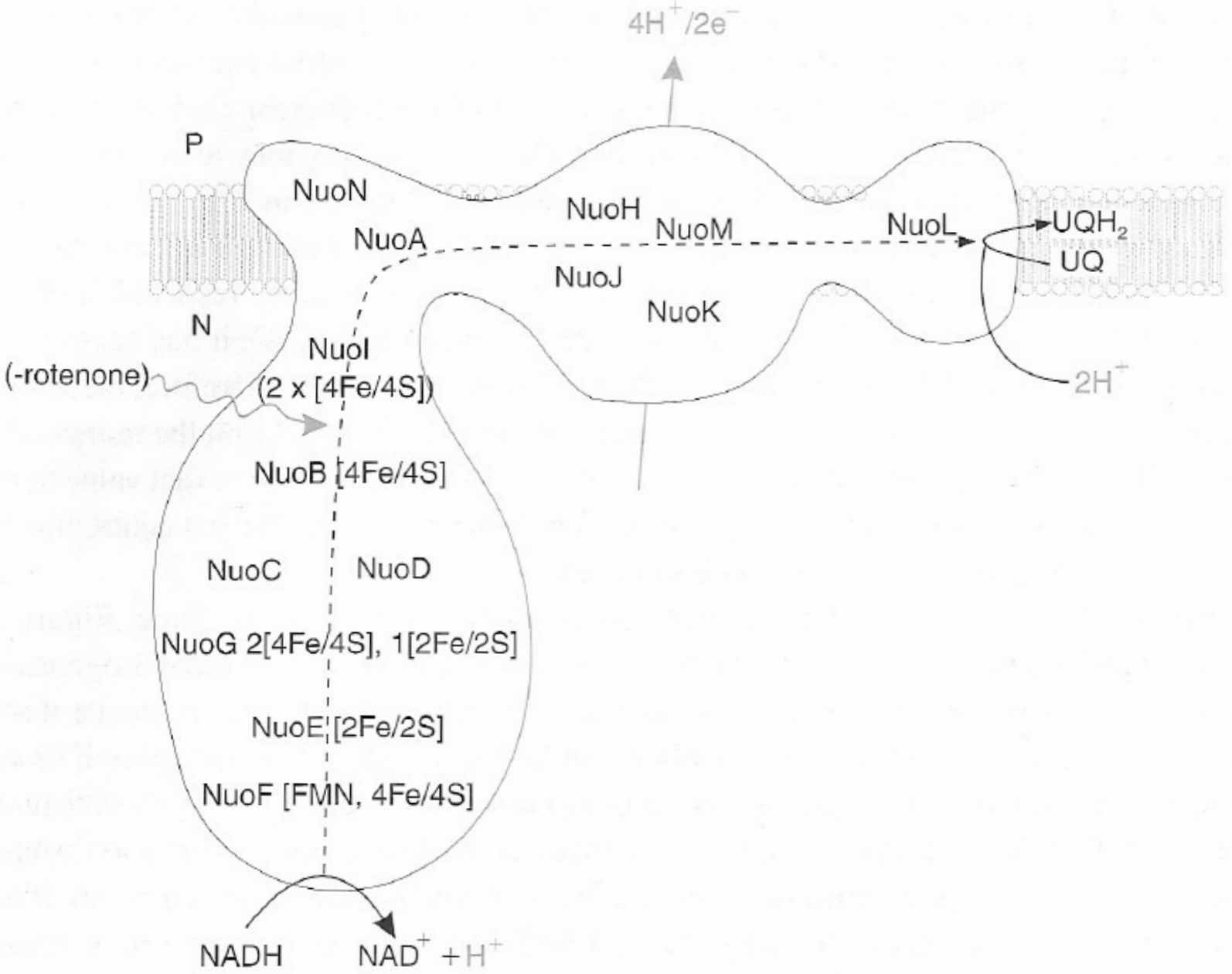

Figure 5.12 An outline structure for the mitochondrial (and bacterial) proton-translocating NADH–ubiquinone oxidoreductase (complex I).

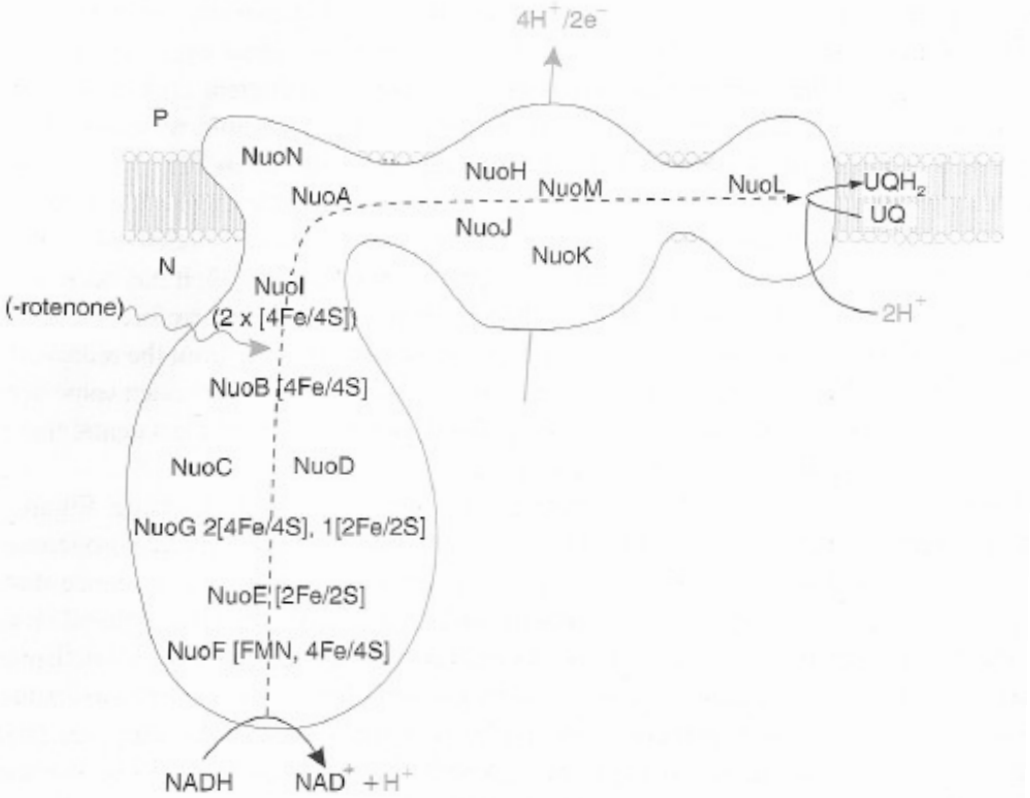

Figure 5.12 An outline structure for the mitochondrial (and bacterial) proton-translocating NADH–ubiquinone oxidoreductase (complex I).
The 14 subunits are named according to one nomenclature system (Nuo) used for the bacterial enzyme. Another bacterial system names the proteins as Nqo (NADH quinone oxidoreductase), whilst the mitochondrial enzyme is named with respect to the approximate molecular weights of the proteins and whether they are assigned to the flavoprotein fraction (FP), the so-called iron protein fraction (IP), stretches of characteristic amino acid sequence, or whether they are coded for on the mitochondrial genome (ND series); the latter are all predicted to be very hydrophobic proteins (and constitute what is sometimes called the hydrophobic fraction (HP) of the mitochondrial enzyme) that do not contain any known redox active groups. The equivalences are:

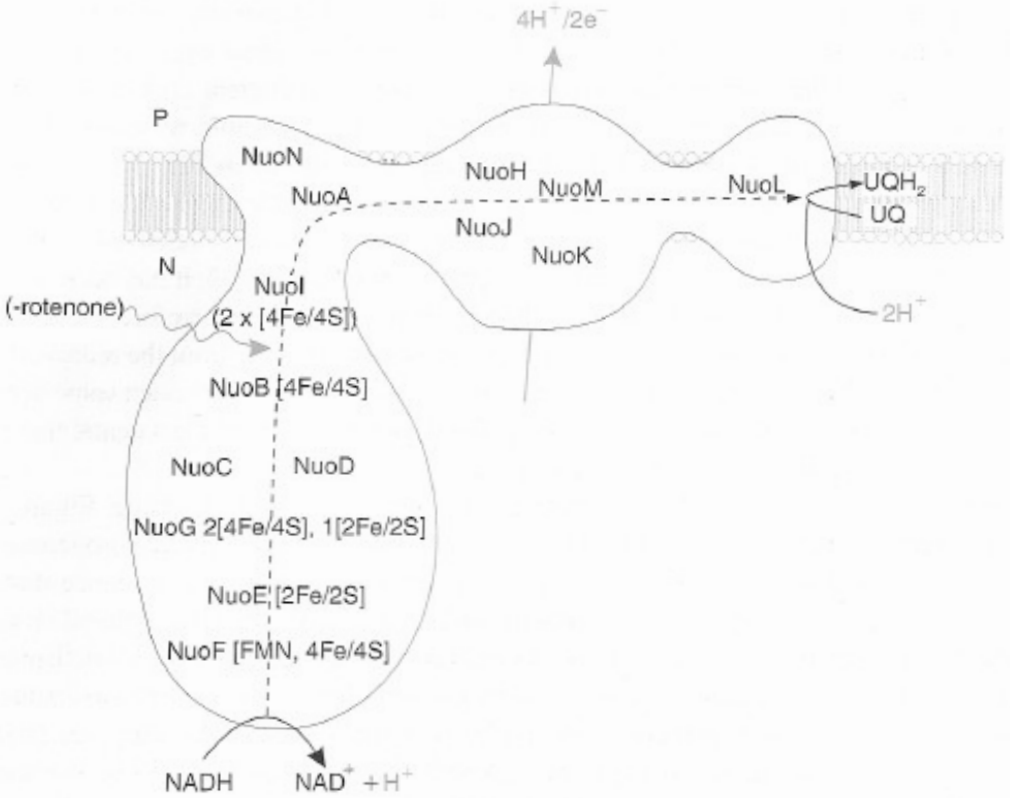

Bacteria		Mitochondria
NuoA	Nqo7	ND3
NuoB	Nqo6	PSST
NuoC	Nqo5	IP30K
NuoD	Nqo4	IP49K
NuoE	Nqo2	FP24K
NuoF	Nqo1	FP51K
NuoG	Nqo3	IP75K
NuoH	Nqo8	ND1
NuoI	Nqo9	TYKY
NuoJ	Nqo10	ND6
NuoK	Nqo11	ND4L
NuoL	Nqo12	ND5
NuoM	Nqo13	ND4
NuoN	Nqo14	ND2

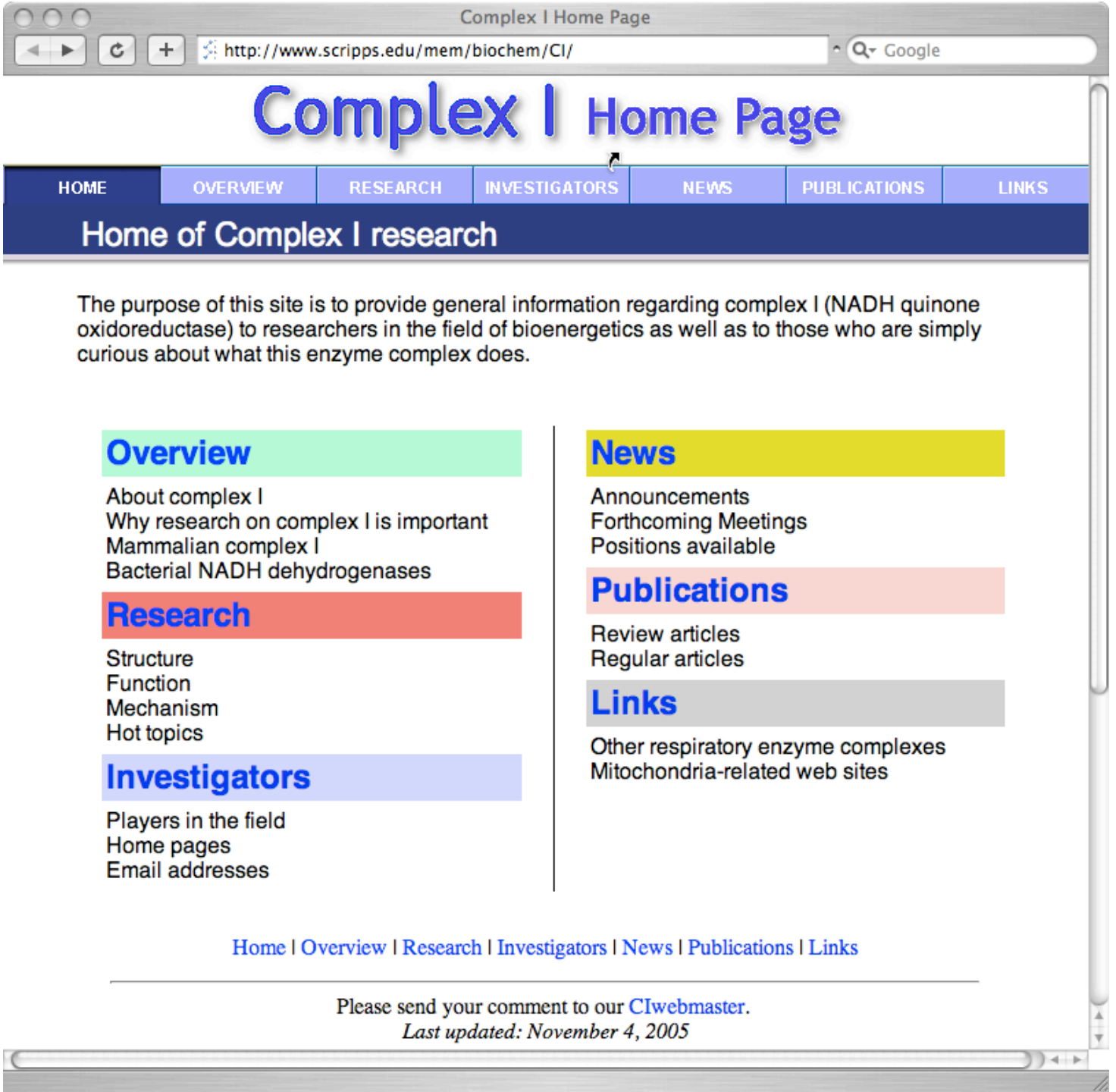
Complex I Home Page
http://www.scripps.edu/mem/biochem/CI/
Google
Complex I Home Page
HOME
OVERVIEW
RESEARCH
INVESTIGATORS
NEWS
PUBLICATIONS
LINKS
Home of Complex I research
The purpose of this site is to provide general information regarding complex I (NADH quinone oxidoreductase) to researchers in the field of bioenergetics as well as to those who are simply curious about what this enzyme complex does.
Overview
About complex I
Why research on complex I is important
Mammalian complex I
Bacterial NADH dehydrogenases
Research
Structure
Function
Mechanism
Hot topics
Investigators
Players in the field
Home pages
Email addresses
News
Announcements
Forthcoming Meetings
Positions available
Publications
Review articles
Regular articles
Links
Other respiratory enzyme complexes
Mitochondria-related web sites
Home | Overview | Research | Investigators | News | Publications | Links
Please send your comment to our CIwebmaster.
Last updated: November 4, 2005

About complex I

The NADH-quinone oxidoreductase (complex I) is one of three energy-transducing enzyme complexes of the respiratory chain in mitochondria. It catalyses the reaction:

$NADH + Q + H^+ + nH^+_{in} \rightarrow NAD^+ + QH_2 + nH^+_{out}$ (Q=quinone; n=3-5)

Complex I is the point of entry for the major fraction of electrons that traverse the respiratory chain eventually resulting in the reduction of oxygen. Coupled to the electron transfer, protons are pumped from the matrix side to the intermembrace space of mitochondria. It is the most intricate membrane-bound enzyme known to date, being composed of at least 46 unlike polypeptides. Of these, 7 are encoded by mitochondrial DNA.

Although four decades have passed since the first isolation of complex I from bovine heart mitochondria by Joe Hatefi and coworkers, information on its structure and mechanism of action is still limited. This enzyme complex contains a noncovalently-bound FMN molecule and 2 binuclear and 6 tetranuclear iron-sulfur clusters, of which 2 binuclear and 4 tetranuclear clusters are EPR-visible.

Why research on complex I is important

Research on complex I has recently taken on greater significance since the finding that many human mitochondrial diseases involve structural and functional defects at the level of this enzyme complex. Many cases of Leber's hereditary optic neuropathy (LHON), appear to be associated with a defect in complex I. The defect identified in many cases is a single nucleotide change in the mitochondrial DNA converting the 340th amino acid of the ND4 subunit of complex I from an arginine to a histidine. In addition to these documented cases, complex I inhibitors, 1-methyl-4-phenylpyridium and rotenone, produce drug-induced Parkinsonism in rodents and human, which suggests a link between Parkinson's disease and function of mitochondrial complex I. Complex I is also known to be a target of new pesticides such as acaricides. Moreover, it is suggested that complex I malfunction is involved in the pathogenesis of diabetes. Therefore, complex I research is important to not only basic sciences but also clinical medicine. This is evident in the progressively growing number of publications relating to complex I, as depicted in the figure. There are several milestones in complex I research. In 1973, Ragan and Racker showed that complex I is a proton pump. In the mid-1980s, it was found that the 7 unidentified genes in mtDNA are encoding complex I subunits by Attardi's group. Shortly after that, the first case of mitochondrial diseases caused by complex I defects was reported (Wallace et al., 1988).

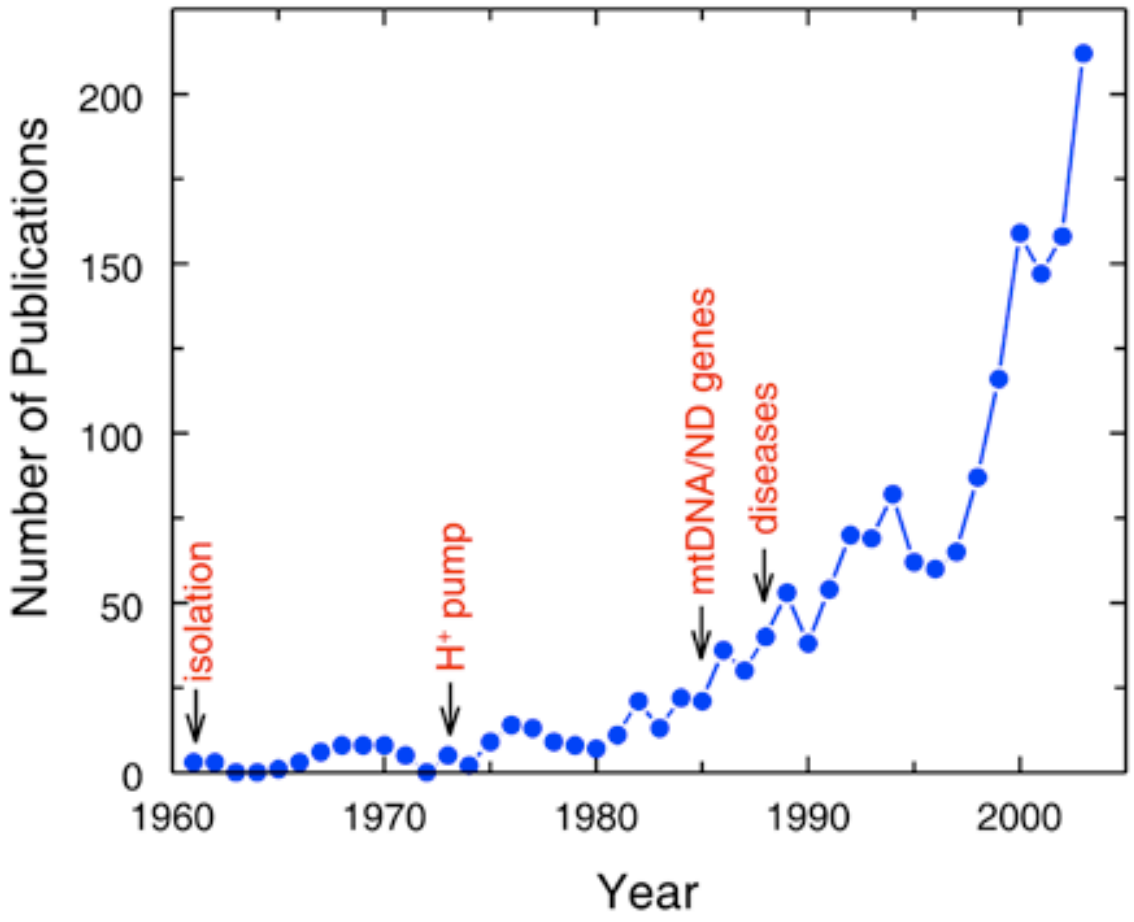

EM images and 3D models of complex I

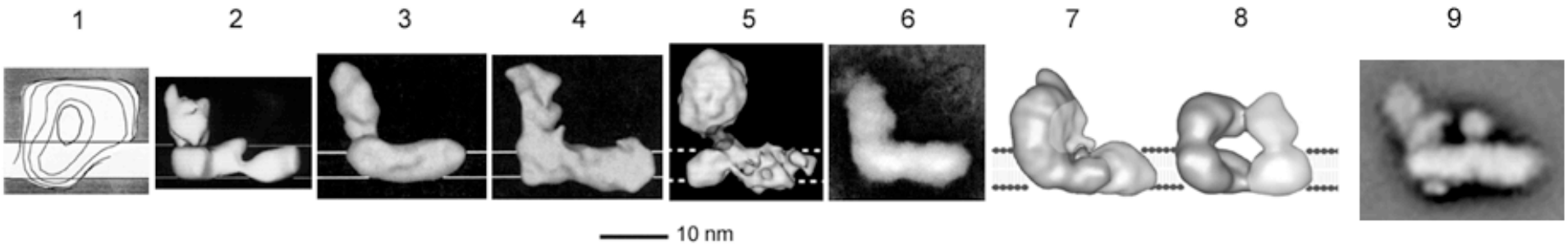

1. *N. crassa*. (Leonard et al., 1987)
2. *N. crassa*. (Hofhaus et al., 1991)
3. *N. crassa* (Guénebaut et al., 1997)
4. *E. coli NDH-1* (Guénebaut et al., 1998)
5. Bovine heart (Grigorieff, 1998)
6. *Y. lipolytica* (Djafarzadeha et al., 2000)

7 and 8. *E. coli* (Böttcher et al., 2002); 7 is "inactive" form, 8 is "active" form

9. *Arabidopsis* (Dudkina et al., 2005)

Relevant papers as pdf files. Please observe copyright

- Structure of the Hydrophilic Domain of Respiratory Complex I from Thermus thermophilus
- Structure of the Hydrophilic Domain of Respiratory Complex I from Thermus thermophilus pdf file
- An atypical haem in the cytochrome b6f complex pdf file
- Structure of the Cytochrome b6f Complex of Oxygenic Photosynthesis: Tuning the Cavity pdf file
- Protein synthesis by isolated pea mitochondria is dependent on the activity of respiratory complex II
- Structure for signalling and vectorial metabolism
- Energy transduction anchors genes in organelles
- The function of genomes in bioenergetic organelles
- Power for life
- Chemiosmotic coupling: The Cost of Living Professor Peter Rich
- Power Games By Nick Lane
- Photosynthesis - telling it like it is Review of Blankenship's Molecular Mechanisms of Photosynthesis

---

Nobel prizes

- 1978 Chemistry Nobel Prize to Peter Mitchell
- 1988 Chemistry Nobel Prize to Johann Deisenhofer, Robert Huber and Hartmut Michel
- 1997 Chemistry Nobel Prize to Paul D. Boyer, John E. Walker and Jens C. Skou

---

John F. Allen web page

Lectures | Membrane Biochemistry | Membrane Proteins | Cell Biology and Developmental Genetics | Inaugural Lecture

---

Structure of the Hydrophilic Domain of Respiratory Complex I from *Thermus thermophilus*

Leonid A. Sazanov* and Philip Hinchliffe

Respiratory complex I plays a central role in cellular energy production in bacteria and mitochondria. Its dysfunction is implicated in many human neurodegenerative diseases, as well as in aging. The crystal structure of the hydrophilic domain (peripheral arm) of complex I from *Thermus thermophilus* has been solved at 3.3 angstrom resolution. This subcomplex consists of eight subunits and contains all the redox centers of the enzyme, including nine iron-sulfur clusters. The primary electron acceptor, flavin-mononucleotide, is within electron transfer distance of cluster N3, leading to the main redox pathway, and of the distal cluster N1a, a possible antioxidant. The structure reveals new aspects of the mechanism and evolution of the enzyme. The terminal cluster N2 is coordinated, uniquely, by two consecutive cysteines. The novel subunit Nqo15 has a similar fold to the mitochondrial iron chaperone frataxin, and it may be involved in iron-sulfur cluster regeneration in the complex.

Complex I [dihydronicotinamide adenine dinucleotide (NADH)–ubiquinone oxidoreductase, EC 1.6.5.3] is the first enzyme of the mitochondrial and bacterial respiratory chains. It catalyzes the transfer of two electrons from NADH to quinone, coupled to the translocation of about four protons across the membrane, helping to provide the proton-motive force required for the synthesis of adenosine triphosphate (ATP) (*1*, *2*). The mitochondrial enzyme contains 46 different subunits (*3*) and is one of the largest known membrane protein complexes. The prokaryotic enzyme is simpler and has 14 subunits with a combined molecular mass of about 550 kD. Analogs of all subunits of bacterial complex I (also referred to as NDH-1) are found in the mitochondrial enzyme (*1*), and they contain equivalent redox components (*2*). Mitochondrial and bacterial enzymes have a characteristic L-shaped structure, with the hydrophobic arm embedded in the membrane and the hydrophilic peripheral arm protruding into the mitochondrial matrix or the bacterial cytoplasm (*4*–*6*). Thus, NDH-1 is a "minimal" model of complex I. Until now, its atomic structure and the mechanism of electron transfer have not been known. Because of its central role in respiration, mutations in subunits of complex I can lead to many human neurodegenerative diseases (*7*). Also, complex I has been suggested to be a major source of reactive oxygen species (ROS) in mitochondria, which can damage mitochondrial DNA and may be one of the causes of aging (*8*).

Medical Research Council Dunn Human Nutrition Unit, Wellcome Trust/MRC Building, Hills Road, Cambridge CB2 2XY, U.K.

*To whom correspondence should be addressed. E-mail: sazanov@mrc-dunn.cam.ac.uk

The hydrophilic domain of complex I contains the NADH-binding site, the flavin-mononucleotide (FMN), and eight or nine iron-sulfur (Fe-S) clusters (*2*, *9*), whereas the proton-pumping machinery is probably in the membrane arm. FMN accepts two electrons simultaneously (as a hydride) from NADH and transfers them one at a time to one-electron carriers, the Fe-S clusters. These subsequently reduce membrane-embedded quinone to quinol in two one-electron steps. In models of the subunit arrangement (*10*–*13*), subunits Nqo1 to 3 form the dehydrogenase domain, and subunits Nqo4 to 6 and Nqo9 connect it to the membrane arm (*Thermus* nomenclature is used throughout, with bovine mitochondrial nomenclature shown in parentheses in section headings). Fe-S clusters identified by electron paramagnetic resonance spectroscopy (EPR) include the binuclear clusters N1a and N1b, and the tetranuclear clusters N2, N3, N4, N5, N6a, and N6b (*2*, *9*). Complex I from *Thermus thermophilus* and from some other bacteria contains the additional tetranuclear cluster N7 (*14*). At pH 7, the two-electron midpoint redox potential of NADH is about –320 mV, of ubiquinone +110 mV (*Thermus* uses menaquinone, –80 mV), and of FMN about –340 mV. The one-electron potential of cluster N1a is about –370 mV and of cluster N2 about –100 mV, and all the other clusters appear to be isopotential at about –250 mV (*2*, *9*). It is likely that cluster N3 accepts electrons from FMN, whereas the high-potential cluster N2 reduces the quinone at the interface with the membrane domain (*1*, *2*, *9*).

We have solved the crystal structure of the hydrophilic domain (peripheral arm) of complex I from *T. thermophilus* HB-8. This subcomplex consists of seven known hydrophilic subunits (Nqo1 to 6 and Nqo9) and a previously unknown subunit, which we have identified as part of the complex and named Nqo15 (*15*, *16*). The domain contains all the redox centers and represents more than half the molecular mass of the entire complex (280 out of 520 kD).

Structure Determination and Overall Architecture

Two heavy atom derivatives were useful in providing phase information [in addition to previous Fe-edge data (*15*)], so that, after density modification, the resolution could be extended to 3.3 Å (*17*). Side chains became clearly visible (fig. S1), and the atomic model was built into the electron density. The model was refined to R_{cryst} = 26.5% and R_{free} = 29.8%, with good stereochemistry (table S1). Some N- and C-terminal residues, as well as a few external loops, were not observed in the density and so were not modeled (*17*). The current model contains 2333 residues (out of 2510 predicted from the sequences), 9 Fe-S clusters, and 1 FMN molecule.

In the overview of the structure shown in Fig. 1A, the peripheral arm of complex I is a Y-shaped assembly about 140 Å high. One uppermost tip of the molecule is formed by the subunits Nqo1 and Nqo2, and the other by the C-terminal domain of Nqo3. The main stem is formed by the N-terminal domain of Nqo3 and the connecting subunits. Its lower part consists of subunits Nqo4 and Nqo6 (which coordinates the terminal Fe-S cluster N2), and it forms an interface with the membrane domain. The overall arrangement of subunits and clusters is consistent with our previous interpretation, apart from the assignment of clusters N4 and N5 in subunit Nqo3 (*15*), which are now reversed (Fig. 1B). The FMN is coordinated by subunit Nqo1 at the deep end of a solvent-exposed cavity containing an apparent NADH-binding site. FMN is within 14 Å, the maximum distance for physiological electron transfer (*18*), of both tetranuclear cluster N3 and binuclear cluster N1a. Thus, electrons can be transferred effectively from the flavin to cluster N3 and then, as judged by shortest edge-to-edge distances (Fig. 1B), through a series of five isopotential clusters to the terminal cluster N2, located next to the likely quinone-binding site. This pathway, NADH-FMN-N3-N1b-N4-N5-N6a-N6b-N2-quinone, is likely to be the main route for electron transfer within the enzyme. Cluster N7, in subunit Nqo3, is too far from the other clusters to accept electrons effectively. As proposed (*15*), binuclear cluster N1a may act as an antioxidant.

At the interface with the membrane domain, subunit Nqo6 contains a rigid (as judged from B-factors) N-terminal α helix H1 (Fig. 1A), involved in crystal contacts. This amphipathic helix protrudes about 25 Å from the complex and has a relatively polar upper surface and a hydrophobic lower surface. It is, therefore, likely to extend into the surface region of the membrane domain. This interpretation is consistent also with the fit of the structure into a low resolution model of the intact *Escherichia coli* complex I, obtained by cryo-electron microscopy (*19*). Thus, helix H1 can help in the orientation of the model relative to the intact complex; the membrane domain is likely to extend in the direction of the N terminus of this helix (to the right in Fig. 1A). Extensive intersubunit contacts are present in the structure (table S2) and are listed in (*17*).

Protein Subunits and Redox Centers

Subunit Nqo1 (51 kD). This subunit contains the NADH-binding site, the primary electron acceptor FMN, cluster N3, and as a whole, it has no significant sequence similarity to any proteins of known structure. The subunit can be separated roughly into four domains (Fig. 2A): an N-terminal domain (residues 7 to 72, *Thermus* numbering throughout) ending with a glycine-rich loop, followed by a Rossman-fold domain (73 to 240), a ubiquitin-like domain (241 to 335) and a C-terminal four-helical bundle containing cluster N3 (336 to 438).

The N-terminal domain wraps around the Rossman-fold domain on the surface of the complex and contains three short α helices. Searches with SSM [secondary structure matching (*20*)] and DALI (*21*) at the European Bioinformatics Institute servers did not reveal significant structural analogs of this domain. Below and in (*17*), alignments performed with SSM are listed, although DALI was used for the initial searches. The N-terminal domain ends with a glycine-rich loop (residues 62 to 72) that was previously suggested to be involved in binding the adenosine diphosphate (ADP) moiety of NADH, as part of a Rossman nucleotide-binding fold (*1*). Indeed, the Rossman fold–like domain is found after this loop, but it is not a classical Rossman fold and it appears to bind FMN, and presumably NADH as well, in a novel mode. Instead of a six-stranded parallel β sheet with a 6, 5, 4, 1, 2, 3 order of strands (*22*), there are only four strands in the order 4, 1, 2, 3, flanked by α helices (Fig. 2A).

In a classical Rossman fold, the loop between the first strand and nascent helix is glycine rich and binds one of the nucleotide phosphate groups. However, in Nqo1, this loop (residues 93 to 102) does not contain glycine; it is mostly shielded from the solvent and interacts with the buried edge of the isoalloxazine ring of FMN. Flavin is bound at the deep end of a solvent-exposed cavity [previously called channel 1 (*13*)], which contains an apparent binding site for NADH (Fig. 3A). FMN interacts mostly with strand four of the parallel β sheet and with loops emerging from strands one and three. It is held in place by a hydrogen-bonding network (*17*) and interacts mainly with residues from a previously predicted flavin-binding domain [residues 175 to 220 (*1*)], but also with residues among those previously suggested to bind NADH [64 to 70 and 90 to 100 (*1*)].

The FMN cavity can accommodate one NADH molecule comfortably, as indicated by manual docking (not shown on figure), and the residues likely to interact with NADH are shown in Fig. 3A. The invariant residues Glu^{87} and Tyr^{100} are exposed to the solvent at the deep end of the cavity and can interact with the nicotinamide carboxyamide. Residues 66 to 69 from the glycine-rich loop can bind the phosphate groups of the substrate. Consistently, our preliminary data obtained from NADH-containing crystals (at about 5 Å resolution), show a strong additional electron density in this area. The invariant Glu^{140} (and/or Glu^{144}) can make hydrogen bonds to the ribose of the adenosine moiety, similar to the aspartate residue conserved in other dehydrogenases (*22*). Notably, the aromatic rings of Phe^{76} and Phe^{305}, near the entrance to the cavity, are nearly parallel and about 8.5 Å apart. These residues are well positioned to coordinate the adenine ring between side chains, by aromatic stacking interactions. If NADH binds as proposed, its nicotinamide ring will be adjacent to the isoalloxazine ring of FMN, which allows hydride transfer. Similar elements of NAD(P)(H) binding are found in other nucleotide-binding proteins, but in different structural environments. All the residues involved in binding FMN and NADH are strongly conserved, which suggests that the binding pocket is conserved. Thus, in complex I, uniquely, a Rossman-fold domain has evolved to bind both FMN and NADH, by the addition of an extra glycine-rich loop at the N terminus.

The subsequent ubiquitin-like domain has a structural role, but it may also be involved in degradation of complex I, as the domain is exposed at the surface near the tip of the molecule (*17*). Finally, the C-terminal domain coordinates cluster N3 and consists of a four-helix bundle. Although this fold is quite common [fold a.24 in SCOP (*23*)], it has not been observed previously to bind Fe-S clusters. The [4Fe-4S] cluster is coordinated in the cubane geometry by Cys^{354}, Cys^{356}, and Cys^{359} from the loop between the first and second helices of the bundle and by Cys^{400} from the loop between the third and fourth helices (fig. S2A).

Subunit Nqo2 (24 kD). This subunit can be divided into two domains: an N-terminal four-helical bundle (residues 3 to 75) (*17*) and a thioredoxin-like C-terminal domain (residues 76 to 180) (Fig. 2B). The N-terminal domain is involved in interactions with subunits Nqo1 and Nqo3. The C-terminal domain coordinates the binuclear cluster N1a and consists of a mixed β sheet flanked by two α helices. It is very similar to the thioredoxin-like [2Fe-2S] ferredoxin from *Aquifex aeolicus* [Protein Data Bank

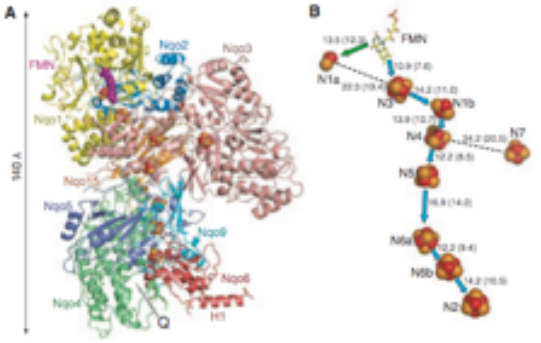

Fig. 1. Architecture of the hydrophilic domain of *T. thermophilus* complex I. **(A)** Side view, with the membrane arm likely to be beneath and extending to the right, in the direction of helix H1. Each subunit is colored differently; FMN is shown as magenta spheres, metal sites as red spheres for Fe atoms and yellow spheres for S atoms. A possible quinone-binding site (Q) is indicated by an arrow. **(B)** Arrangement of redox centers. The overall orientation is similar to that in (A), tilted to provide an improved view of the FMN and the clusters. Cluster N1a is in subunit Nqo2; N3 and FMN in Nqo1; N1b, N4, N5, and N7 in Nqo3; N6a/b in Nqo9; and N2 in Nqo6. The main pathway of electron transfer is indicated by blue arrows, and a diversion to cluster N1a by a green arrow. The distances between the centers given in angstroms were calculated both center-to-center and edge-to-edge (shown in parentheses). Clusters N3 and N4 are separated by 17.6 Å (13.8 Å edge-to-edge), and clusters N1b and N5 by 19.2 Å (16.7 Å edge-to-edge).

Downloaded from www.sciencemag.org on November 16, 2007

RESEARCH ARTICLE

Structure of the Hydrophilic Domain of Respiratory Complex I from *Thermus thermophilus*

Leonid A. Sazanov* and Philip Hinchliffe

Respiratory complex I plays a central role in cellular energy production in bacteria and mitochondria. Its dysfunction is implicated in many human neurodegenerative diseases, as well as in aging. The crystal structure of the hydrophilic domain (peripheral arm) of complex I from *Thermus thermophilus* has been solved at 3.3 angstrom resolution. This subcomplex consists of eight subunits and contains all the redox centers of the enzyme, including nine iron-sulfur clusters. The primary electron acceptor, flavin-mononucleotide, is within electron transfer distance of cluster N3, leading to the main redox pathway, and of the distal cluster N1a, a possible antioxidant. The structure reveals new aspects of the mechanism and evolution of the enzyme. The terminal cluster N2 is coordinated, uniquely, by two consecutive cysteines. The novel subunit Nqo15 has a similar fold to the mitochondrial iron chaperone frataxin, and it may be involved in iron-sulfur cluster regeneration in the complex.

Structure of the Hydrophilic Domain of Respiratory Complex I from *Thermus thermophilus*

Leonid A. Sazanov* and Philip Hinchliffe

Respiratory complex I plays a central role in cellular energy production in bacteria and mitochondria. Its dysfunction is implicated in many human neurodegenerative diseases, as well as in aging. The crystal structure of the hydrophilic domain (peripheral arm) of complex I from *Thermus thermophilus* has been solved at 3.3 angstrom resolution. This subcomplex consists of eight subunits and contains all the redox centers of the enzyme, including nine iron-sulfur clusters. The primary electron acceptor, flavin-mononucleotide, is within electron transfer distance of cluster N3, leading to the main redox pathway, and of the distal cluster N1a, a possible antioxidant. The structure reveals new aspects of the mechanism and evolution of the enzyme. The terminal cluster N2 is coordinated, uniquely, by two consecutive cysteines. The novel subunit Nqo15 has a similar fold to the mitochondrial iron chaperone frataxin, and it may be involved in iron-sulfur cluster regeneration in the complex.

Medical Research Council Dunn Human Nutrition Unit, Wellcome Trust/MRC Building, Hills Road, Cambridge CB2 2XY, U.K.

Hot news on the 3D structure: Hinchliffe and Sazanov recently reported the arrangement of iron-sulfur clusters in the hydrophilic domain of complex I from *Thermus thermophilus* as determined by x-ray crystallography.

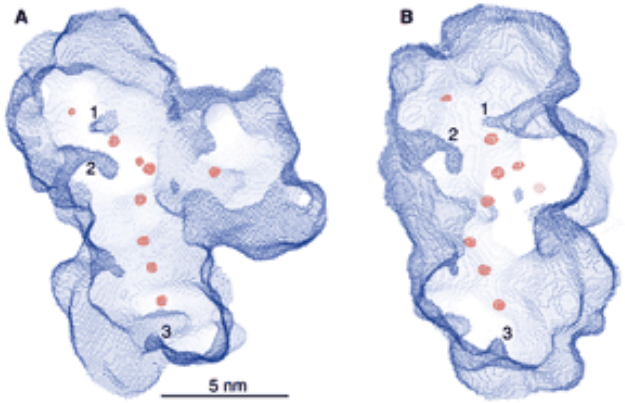

The electron density of Fe-S clusters shown within the molecular surface of the peripheral arm

Reference: Hinchliffe, P. and Sazanov, L. A. (2005) **Organization of iron-sulfur clusters in respiratory complex I**. *Science* **309**:771-774.

Hot news on the 3D structure: Hinchliffe and Sazanov recently reported the arrangement of iron-sulfur clusters in the hydrophilic domain of complex I from *Thermus thermophilus* as determined by x-ray crystallography.

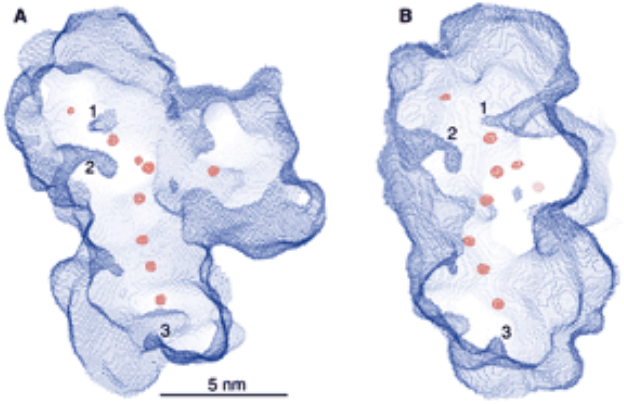

The electron density of Fe-S clusters shown within the molecular surface of the peripheral arm

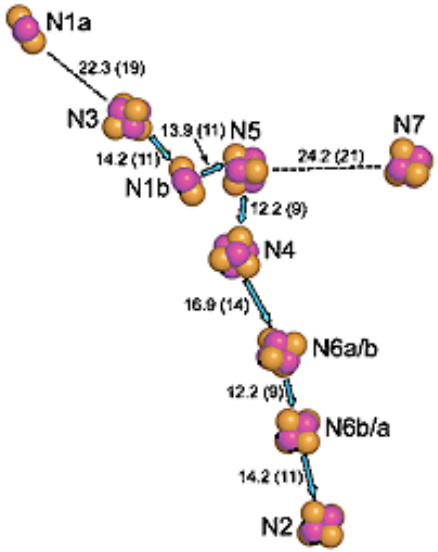

Arrangement of Fe-S clusters in complex I

Reference: Hinchliffe, P. and Sazanov, L. A. (2005) **Organization of iron-sulfur clusters in respiratory complex I**. *Science* **309**:771-774. Reprinted with permissions from AAAS. Permission from AAAS is required for all other uses.

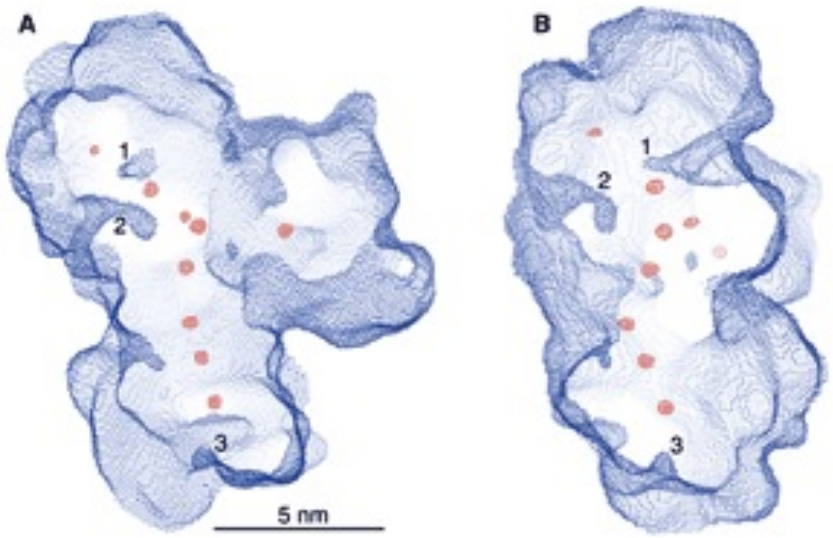

The electron density of Fe-S clusters shown within the molecular surface of the peripheral arm

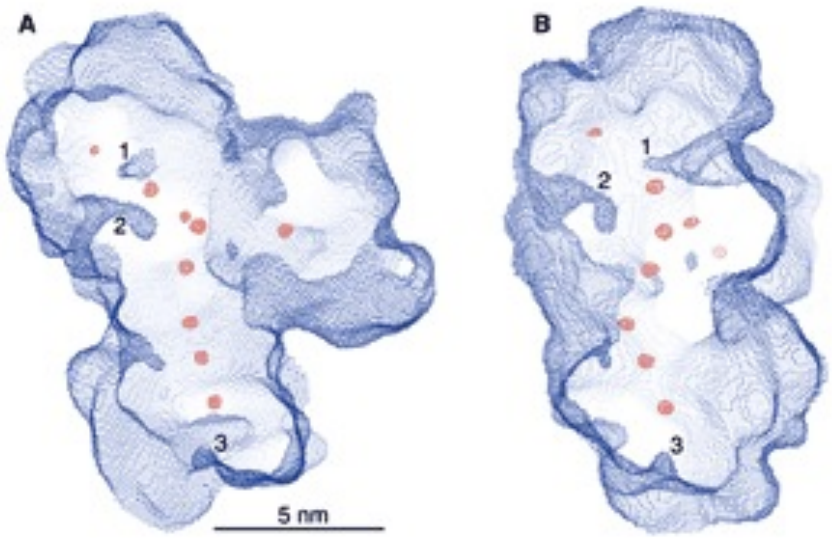

The electron density of Fe-S clusters shown within the molecular surface of the peripheral arm

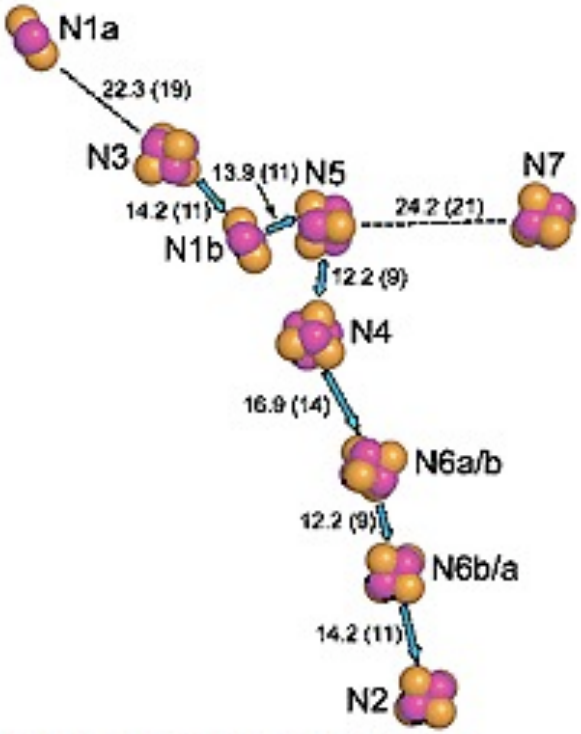

Arrangement of Fe-S clusters in complex I

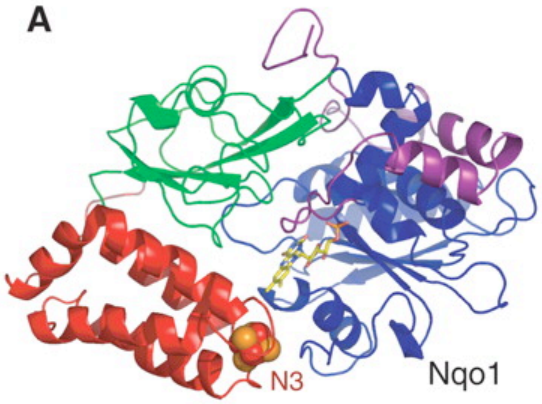

Fig. 2. The folds of individual subunits. Fe-S centers are shown as red spheres for Fe atoms and yellow spheres for S atoms, with cluster names in red. Subunits are not drawn to the same scale. (**A**) Nqo1. Its N-terminal domain is in purple, a Rossman-fold domain in blue, an ubiquitin-like domain in green, and the C-terminal helical bundle, coordinating cluster N3, in red. FMN is shown in stick representation. (**B**) Nqo2. The N-terminal helical bundle is shown in blue, the thioredoxin-like domain coordinating cluster N1a in green. (**C**) Nqo3. The N-terminal [FeFe]-hydrogenase–like domain coordinating clusters N1b, N4, and N5 is magenta, subdomains of the C-terminal molybdoenzyme-like domain are shown in I (coordinating cluster N7), blue; II, green; III, yellow; and IV, red. (**D**) Nqo9, coordinating clusters N6a and N6b, is shown in rainbow representation, colored blue to red from N to C terminus. (**E**) Nqo6, coordinating cluster N2, is shown in rainbow representation, with helix H1 indicated. (**F**) Nqo4. The N-terminal ß domain is shown in blue, the -helical bundle in green, the extended helix H2 in yellow, and the C-terminal ß domain in orange. Clusters are shown for orientation only. (**G**) Nqo5. The N-terminal /ß domain interacting with Nqo4 is shown in blue, the domain interacting with Nqo9 in green, and the C-terminal loop interacting with Nqo3 in yellow. Clusters are shown for orientation only. (**H**) Nqo15, shown in rainbow representation. The histidines exposed inside the putative iron storage cavity are shown.

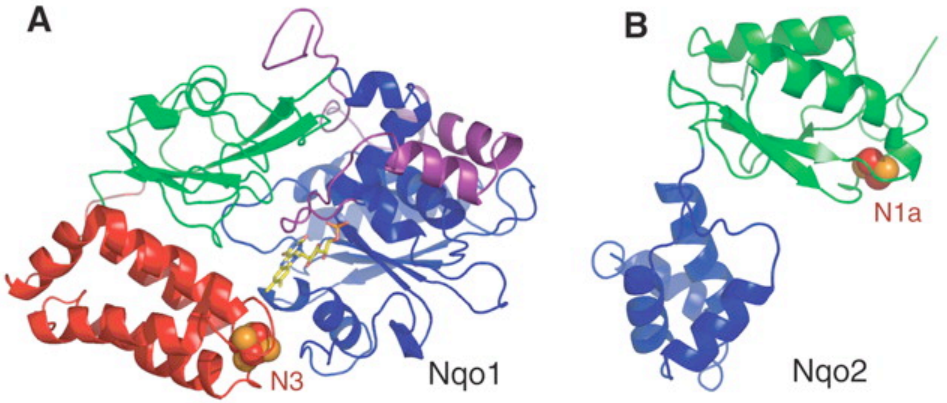

Fig. 2. The folds of individual subunits. Fe-S centers are shown as red spheres for Fe atoms and yellow spheres for S atoms, with cluster names in red. Subunits are not drawn to the same scale. (**A**) Nqo1. Its N-terminal domain is in purple, a Rossman-fold domain in blue, an ubiquitin-like domain in green, and the C-terminal helical bundle, coordinating cluster N3, in red. FMN is shown in stick representation. (**B**) Nqo2. The N-terminal helical bundle is shown in blue, the thioredoxin-like domain coordinating cluster N1a in green. (**C**) Nqo3. The N-terminal [FeFe]-hydrogenase–like domain coordinating clusters N1b, N4, and N5 is magenta, subdomains of the C-terminal molybdoenzyme-like domain are shown in I (coordinating cluster N7), blue; II, green; III, yellow; and IV, red. (**D**) Nqo9, coordinating clusters N6a and N6b, is shown in rainbow representation, colored blue to red from N to C terminus. (**E**) Nqo6, coordinating cluster N2, is shown in rainbow representation, with helix H1 indicated. (**F**) Nqo4. The N-terminal ß domain is shown in blue, the -helical bundle in green, the extended helix H2 in yellow, and the C-terminal ß domain in orange. Clusters are shown for orientation only. (**G**) Nqo5. The N-terminal /ß domain interacting with Nqo4 is shown in blue, the domain interacting with Nqo9 in green, and the C-terminal loop interacting with Nqo3 in yellow. Clusters are shown for orientation only. (**H**) Nqo15, shown in rainbow representation. The histidines exposed inside the putative iron storage cavity are shown.

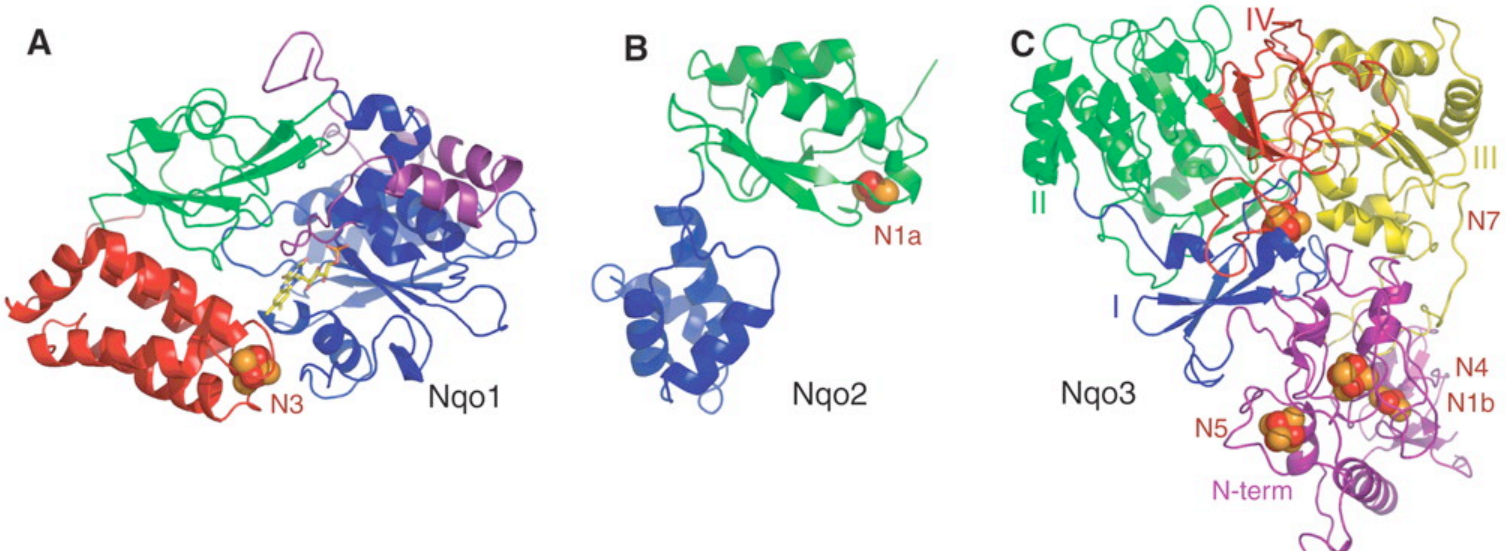

Fig. 2. The folds of individual subunits. Fe-S centers are shown as red spheres for Fe atoms and yellow spheres for S atoms, with cluster names in red. Subunits are not drawn to the same scale. (**A**) Nqo1. Its N-terminal domain is in purple, a Rossman-fold domain in blue, an ubiquitin-like domain in green, and the C-terminal helical bundle, coordinating cluster N3, in red. FMN is shown in stick representation. (**B**) Nqo2. The N-terminal helical bundle is shown in blue, the thioredoxin-like domain coordinating cluster N1a in green. (**C**) Nqo3. The N-terminal [FeFe]-hydrogenase–like domain coordinating clusters N1b, N4, and N5 is magenta, subdomains of the C-terminal molybdoenzyme-like domain are shown in I (coordinating cluster N7), blue; II, green; III, yellow; and IV, red. (**D**) Nqo9, coordinating clusters N6a and N6b, is shown in rainbow representation, colored blue to red from N to C terminus. (**E**) Nqo6, coordinating cluster N2, is shown in rainbow representation, with helix H1 indicated. (**F**) Nqo4. The N-terminal ß domain is shown in blue, the -helical bundle in green, the extended helix H2 in yellow, and the C-terminal ß domain in orange. Clusters are shown for orientation only. (**G**) Nqo5. The N-terminal /ß domain interacting with Nqo4 is shown in blue, the domain interacting with Nqo9 in green, and the C-terminal loop interacting with Nqo3 in yellow. Clusters are shown for orientation only. (**H**) Nqo15, shown in rainbow representation. The histidines exposed inside the putative iron storage cavity are shown.

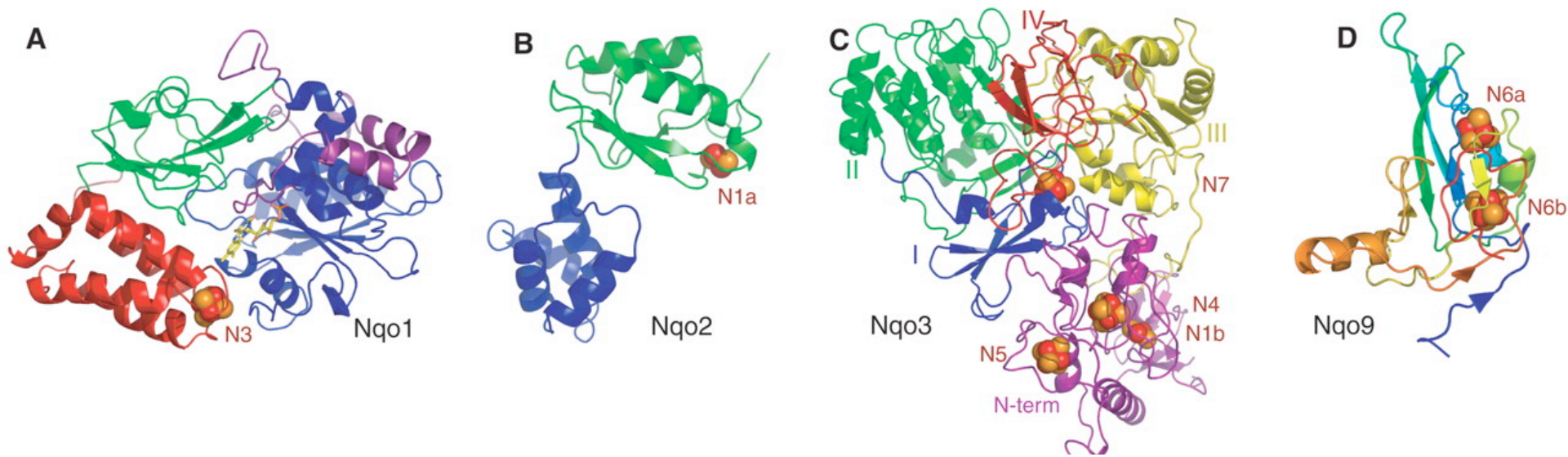

Fig. 2. The folds of individual subunits. Fe-S centers are shown as red spheres for Fe atoms and yellow spheres for S atoms, with cluster names in red. Subunits are not drawn to the same scale. (**A**) Nqo1. Its N-terminal domain is in purple, a Rossman-fold domain in blue, an ubiquitin-like domain in green, and the C-terminal helical bundle, coordinating cluster N3, in red. FMN is shown in stick representation. (**B**) Nqo2. The N-terminal helical bundle is shown in blue, the thioredoxin-like domain coordinating cluster N1a in green. (**C**) Nqo3. The N-terminal [FeFe]-hydrogenase–like domain coordinating clusters N1b, N4, and N5 is magenta, subdomains of the C-terminal molybdoenzyme-like domain are shown in I (coordinating cluster N7), blue; II, green; III, yellow; and IV, red. (**D**) Nqo9, coordinating clusters N6a and N6b, is shown in rainbow representation, colored blue to red from N to C terminus. (**E**) Nqo6, coordinating cluster N2, is shown in rainbow representation, with helix H1 indicated. (**F**) Nqo4. The N-terminal ß domain is shown in blue, the -helical bundle in green, the extended helix H2 in yellow, and the C-terminal ß domain in orange. Clusters are shown for orientation only. (**G**) Nqo5. The N-terminal /ß domain interacting with Nqo4 is shown in blue, the domain interacting with Nqo9 in green, and the C-terminal loop interacting with Nqo3 in yellow. Clusters are shown for orientation only. (**H**) Nqo15, shown in rainbow representation. The histidines exposed inside the putative iron storage cavity are shown.

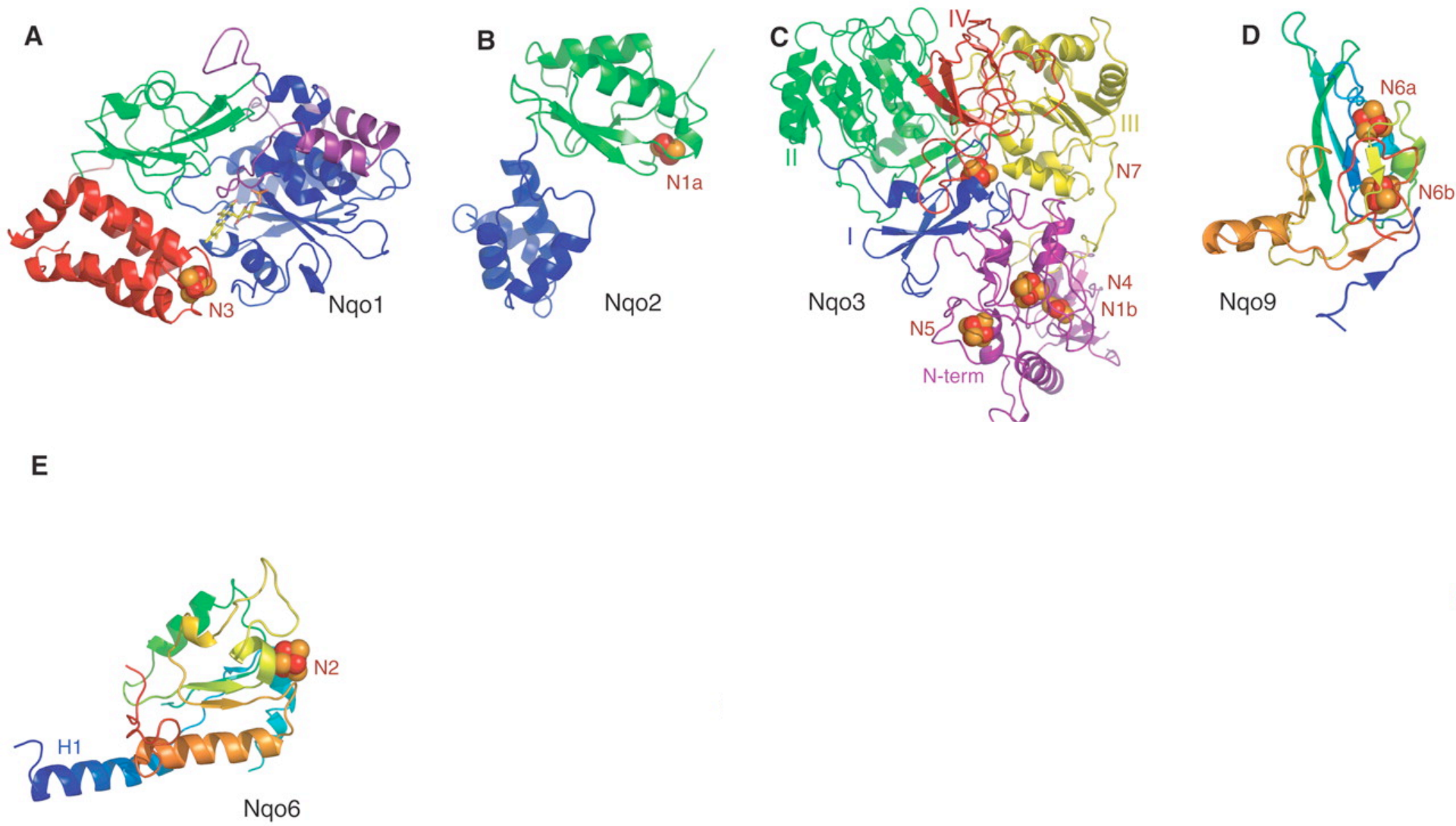

Fig. 2. The folds of individual subunits. Fe-S centers are shown as red spheres for Fe atoms and yellow spheres for S atoms, with cluster names in red. Subunits are not drawn to the same scale. (**A**) Nqo1. Its N-terminal domain is in purple, a Rossman-fold domain in blue, an ubiquitin-like domain in green, and the C-terminal helical bundle, coordinating cluster N3, in red. FMN is shown in stick representation. (**B**) Nqo2. The N-terminal helical bundle is shown in blue, the thioredoxin-like domain coordinating cluster N1a in green. (**C**) Nqo3. The N-terminal [FeFe]-hydrogenase–like domain coordinating clusters N1b, N4, and N5 is magenta, subdomains of the C-terminal molybdoenzyme-like domain are shown in I (coordinating cluster N7), blue; II, green; III, yellow; and IV, red. (**D**) Nqo9, coordinating clusters N6a and N6b, is shown in rainbow representation, colored blue to red from N to C terminus. (**E**) Nqo6, coordinating cluster N2, is shown in rainbow representation, with helix H1 indicated. (**F**) Nqo4. The N-terminal ß domain is shown in blue, the -helical bundle in green, the extended helix H2 in yellow, and the C-terminal ß domain in orange. Clusters are shown for orientation only. (**G**) Nqo5. The N-terminal /ß domain interacting with Nqo4 is shown in blue, the domain interacting with Nqo9 in green, and the C-terminal loop interacting with Nqo3 in yellow. Clusters are shown for orientation only. (**H**) Nqo15, shown in rainbow representation. The histidines exposed inside the putative iron storage cavity are shown.

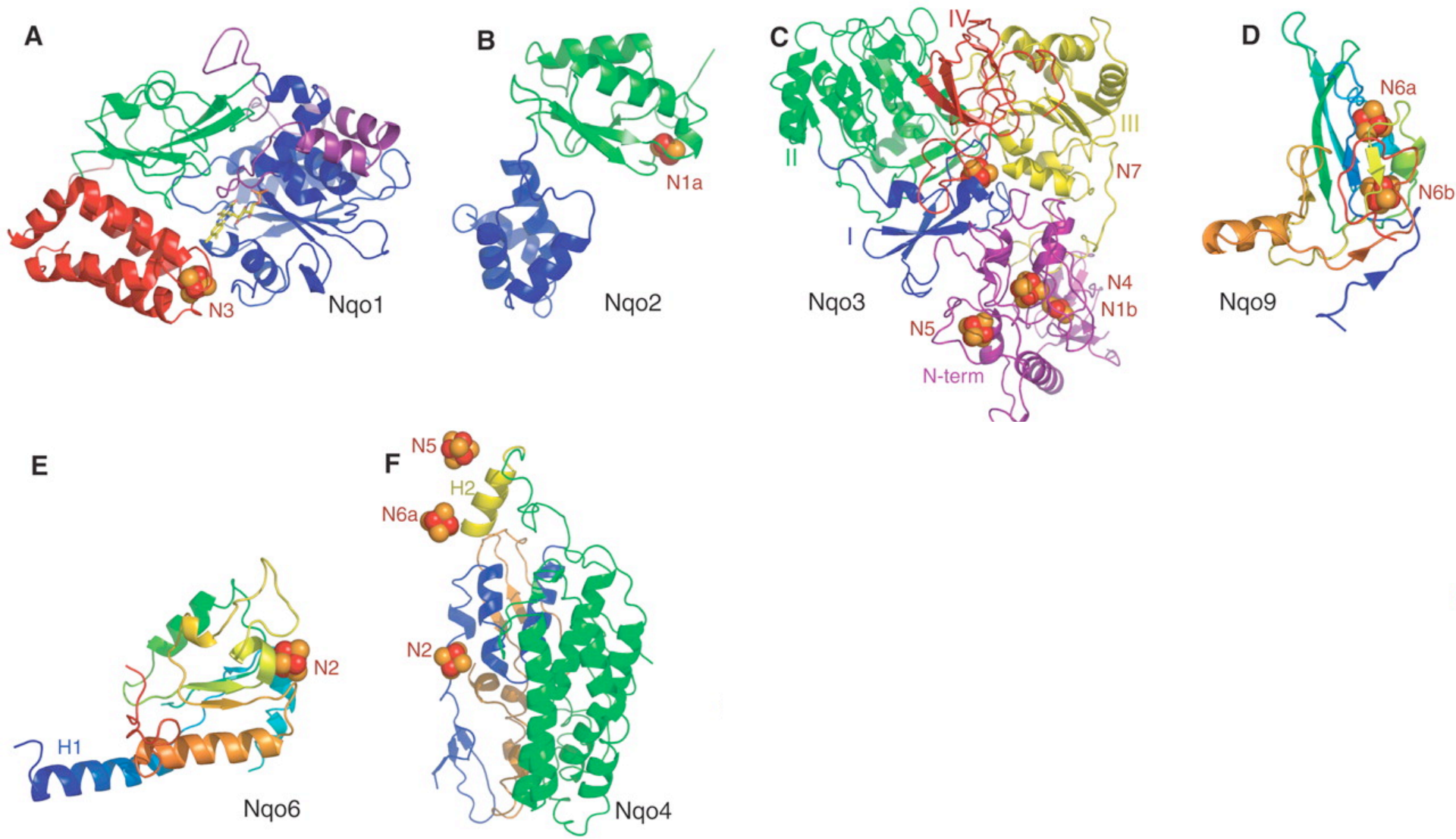

Fig. 2. The folds of individual subunits. Fe-S centers are shown as red spheres for Fe atoms and yellow spheres for S atoms, with cluster names in red. Subunits are not drawn to the same scale. (**A**) Nqo1. Its N-terminal domain is in purple, a Rossman-fold domain in blue, an ubiquitin-like domain in green, and the C-terminal helical bundle, coordinating cluster N3, in red. FMN is shown in stick representation. (**B**) Nqo2. The N-terminal helical bundle is shown in blue, the thioredoxin-like domain coordinating cluster N1a in green. (**C**) Nqo3. The N-terminal [FeFe]-hydrogenase–like domain coordinating clusters N1b, N4, and N5 is magenta, subdomains of the C-terminal molybdoenzyme-like domain are shown in I (coordinating cluster N7), blue; II, green; III, yellow; and IV, red. (**D**) Nqo9, coordinating clusters N6a and N6b, is shown in rainbow representation, colored blue to red from N to C terminus. (**E**) Nqo6, coordinating cluster N2, is shown in rainbow representation, with helix H1 indicated. (**F**) Nqo4. The N-terminal ß domain is shown in blue, the -helical bundle in green, the extended helix H2 in yellow, and the C-terminal ß domain in orange. Clusters are shown for orientation only. (**G**) Nqo5. The N-terminal /ß domain interacting with Nqo4 is shown in blue, the domain interacting with Nqo9 in green, and the C-terminal loop interacting with Nqo3 in yellow. Clusters are shown for orientation only. (**H**) Nqo15, shown in rainbow representation. The histidines exposed inside the putative iron storage cavity are shown.

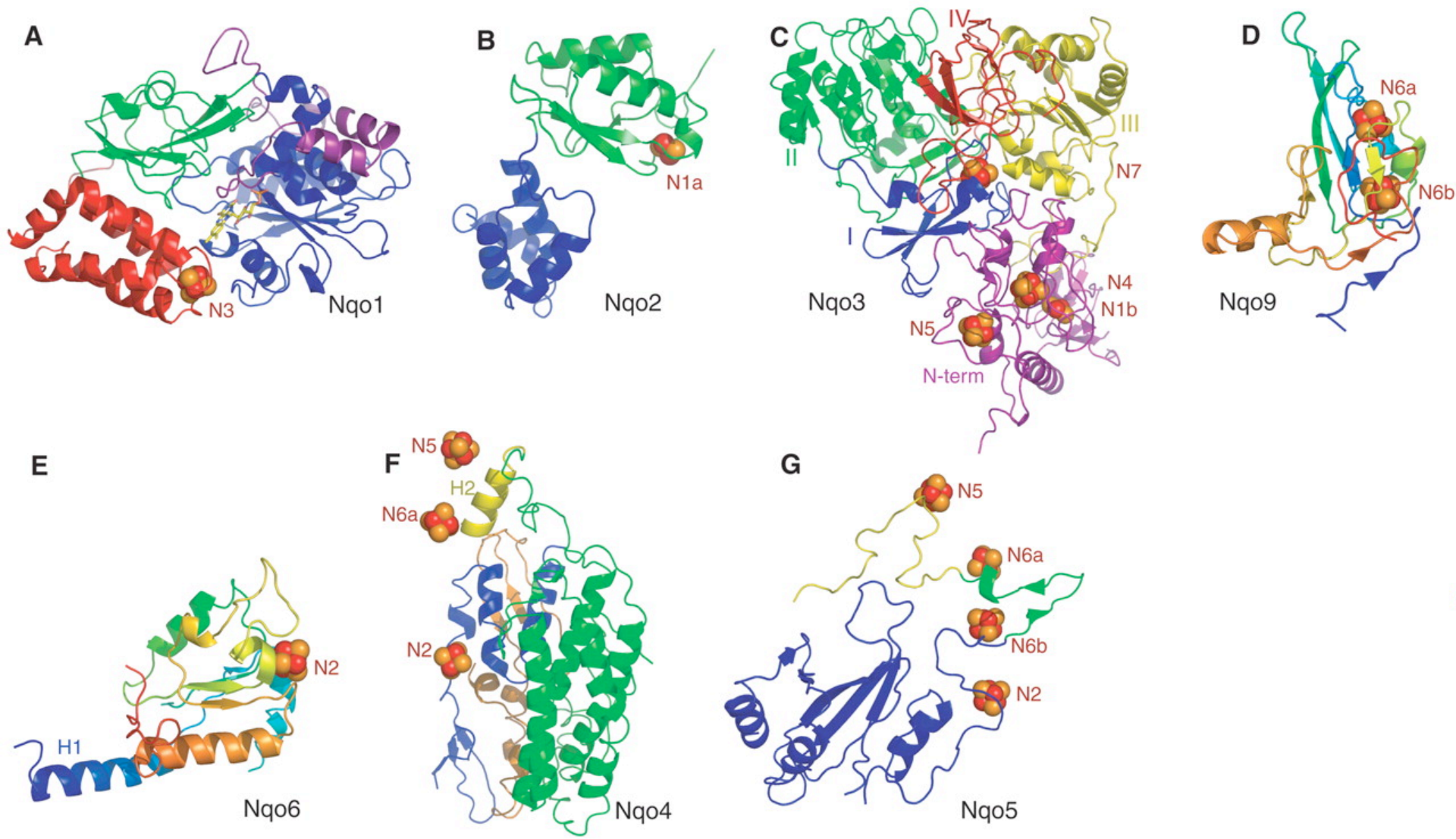

Fig. 2. The folds of individual subunits. Fe-S centers are shown as red spheres for Fe atoms and yellow spheres for S atoms, with cluster names in red. Subunits are not drawn to the same scale. (**A**) Nqo1. Its N-terminal domain is in purple, a Rossman-fold domain in blue, an ubiquitin-like domain in green, and the C-terminal helical bundle, coordinating cluster N3, in red. FMN is shown in stick representation. (**B**) Nqo2. The N-terminal helical bundle is shown in blue, the thioredoxin-like domain coordinating cluster N1a in green. (**C**) Nqo3. The N-terminal [FeFe]-hydrogenase–like domain coordinating clusters N1b, N4, and N5 is magenta, subdomains of the C-terminal molybdoenzyme-like domain are shown in I (coordinating cluster N7), blue; II, green; III, yellow; and IV, red. (**D**) Nqo9, coordinating clusters N6a and N6b, is shown in rainbow representation, colored blue to red from N to C terminus. (**E**) Nqo6, coordinating cluster N2, is shown in rainbow representation, with helix H1 indicated. (**F**) Nqo4. The N-terminal ß domain is shown in blue, the -helical bundle in green, the extended helix H2 in yellow, and the C-terminal ß domain in orange. Clusters are shown for orientation only. (**G**) Nqo5. The N-terminal /ß domain interacting with Nqo4 is shown in blue, the domain interacting with Nqo9 in green, and the C-terminal loop interacting with Nqo3 in yellow. Clusters are shown for orientation only. (**H**) Nqo15, shown in rainbow representation. The histidines exposed inside the putative iron storage cavity are shown.

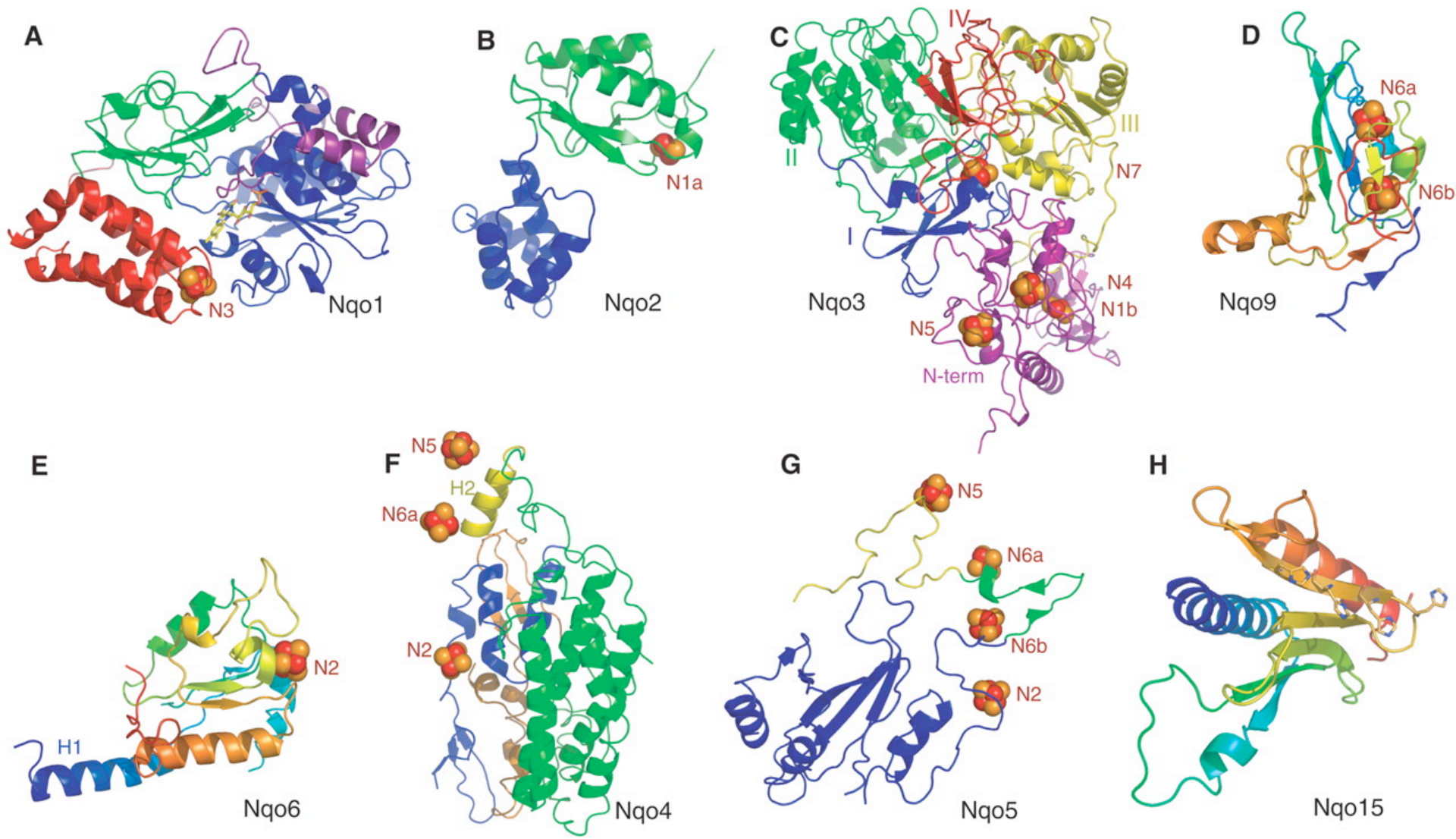

Fig. 2. The folds of individual subunits. Fe-S centers are shown as red spheres for Fe atoms and yellow spheres for S atoms, with cluster names in red. Subunits are not drawn to the same scale. (**A**) Nqo1. Its N-terminal domain is in purple, a Rossman-fold domain in blue, an ubiquitin-like domain in green, and the C-terminal helical bundle, coordinating cluster N3, in red. FMN is shown in stick representation. (**B**) Nqo2. The N-terminal helical bundle is shown in blue, the thioredoxin-like domain coordinating cluster N1a in green. (**C**) Nqo3. The N-terminal [FeFe]-hydrogenase–like domain coordinating clusters N1b, N4, and N5 is magenta, subdomains of the C-terminal molybdoenzyme-like domain are shown in I (coordinating cluster N7), blue; II, green; III, yellow; and IV, red. (**D**) Nqo9, coordinating clusters N6a and N6b, is shown in rainbow representation, colored blue to red from N to C terminus. (**E**) Nqo6, coordinating cluster N2, is shown in rainbow representation, with helix H1 indicated. (**F**) Nqo4. The N-terminal ß domain is shown in blue, the -helical bundle in green, the extended helix H2 in yellow, and the C-terminal ß domain in orange. Clusters are shown for orientation only. (**G**) Nqo5. The N-terminal /ß domain interacting with Nqo4 is shown in blue, the domain interacting with Nqo9 in green, and the C-terminal loop interacting with Nqo3 in yellow. Clusters are shown for orientation only. (**H**) Nqo15, shown in rainbow representation. The histidines exposed inside the putative iron storage cavity are shown.

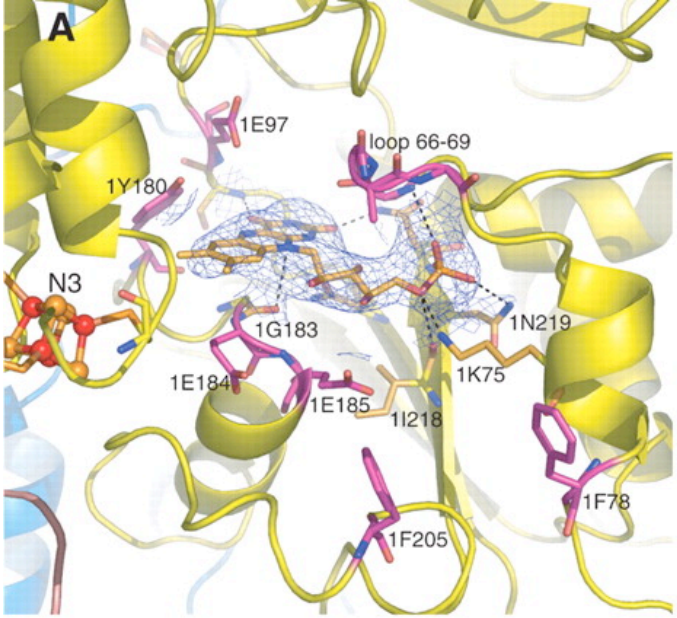

Fig. 3. The environments of the FMN-binding site and of selected Fe-S clusters. (**A**) The binding site for FMN and NADH, viewed from the solvent-exposed side. Residues involved in FMN binding are shown in stick representation with carbon in yellow and hydrogen bonds as dotted lines. Residues likely to be involved in NADH binding are shown in stick representation, with carbon in magenta. Prefixes to residue names indicate the subunit number. Cluster N3 is visible to the left. Subunits are colored as in Fig. 1. A $_{A}$-weighted $2F_{obs} - F_{calc}$ map contoured at 1 is shown around the FMN. (**B**) Cluster N5 and (**C**) cluster N2. Cluster ligands and polar residues nearby are shown. The backbones of subunits are colored as in Fig. 1. Electron density is from a $_{A}$-weighted $2F_{obs} - F_{calc}$ map contoured at 1. Clusters are shown as spheres of 0.3 van der Waals radius.

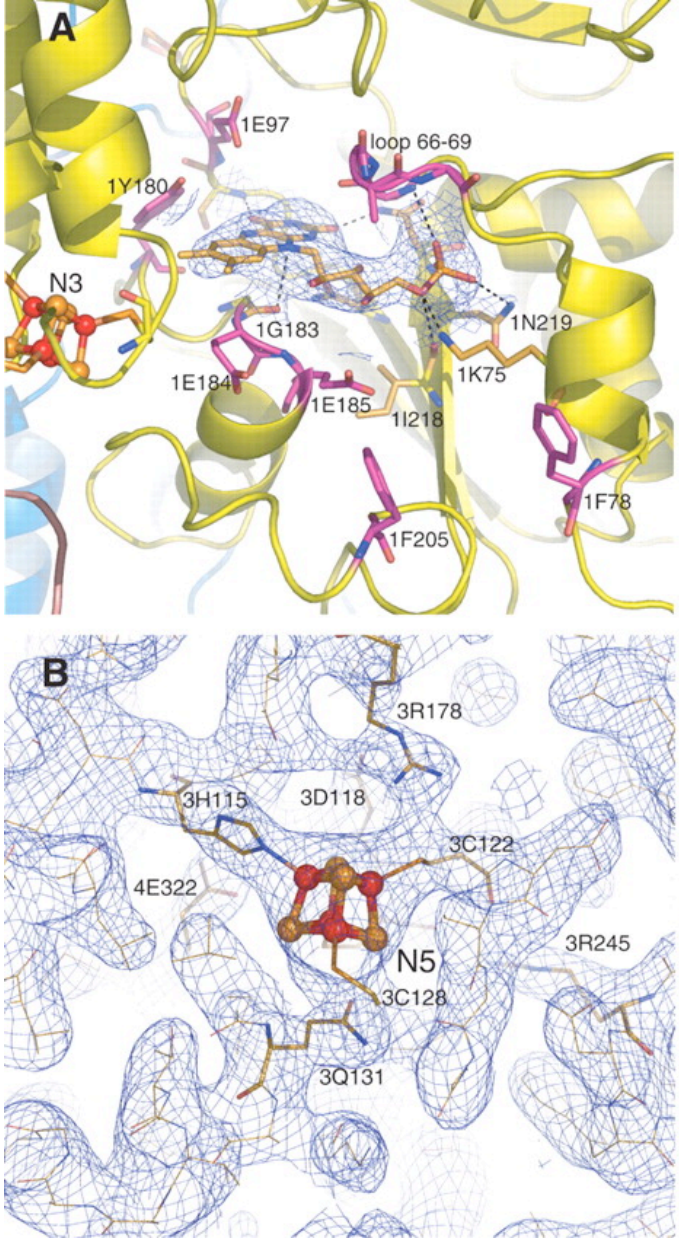

Fig. 3. The environments of the FMN-binding site and of selected Fe-S clusters. (**A**) The binding site for FMN and NADH, viewed from the solvent-exposed side. Residues involved in FMN binding are shown in stick representation with carbon in yellow and hydrogen bonds as dotted lines. Residues likely to be involved in NADH binding are shown in stick representation, with carbon in magenta. Prefixes to residue names indicate the subunit number. Cluster N3 is visible to the left. Subunits are colored as in Fig. 1. A $_{A}$-weighted $2F_{obs} - F_{calc}$ map contoured at 1 is shown around the FMN. (**B**) Cluster N5 and (**C**) cluster N2. Cluster ligands and polar residues nearby are shown. The backbones of subunits are colored as in Fig. 1. Electron density is from a $_{A}$-weighted $2F_{obs} - F_{calc}$ map contoured at 1. Clusters are shown as spheres of 0.3 van der Waals radius.

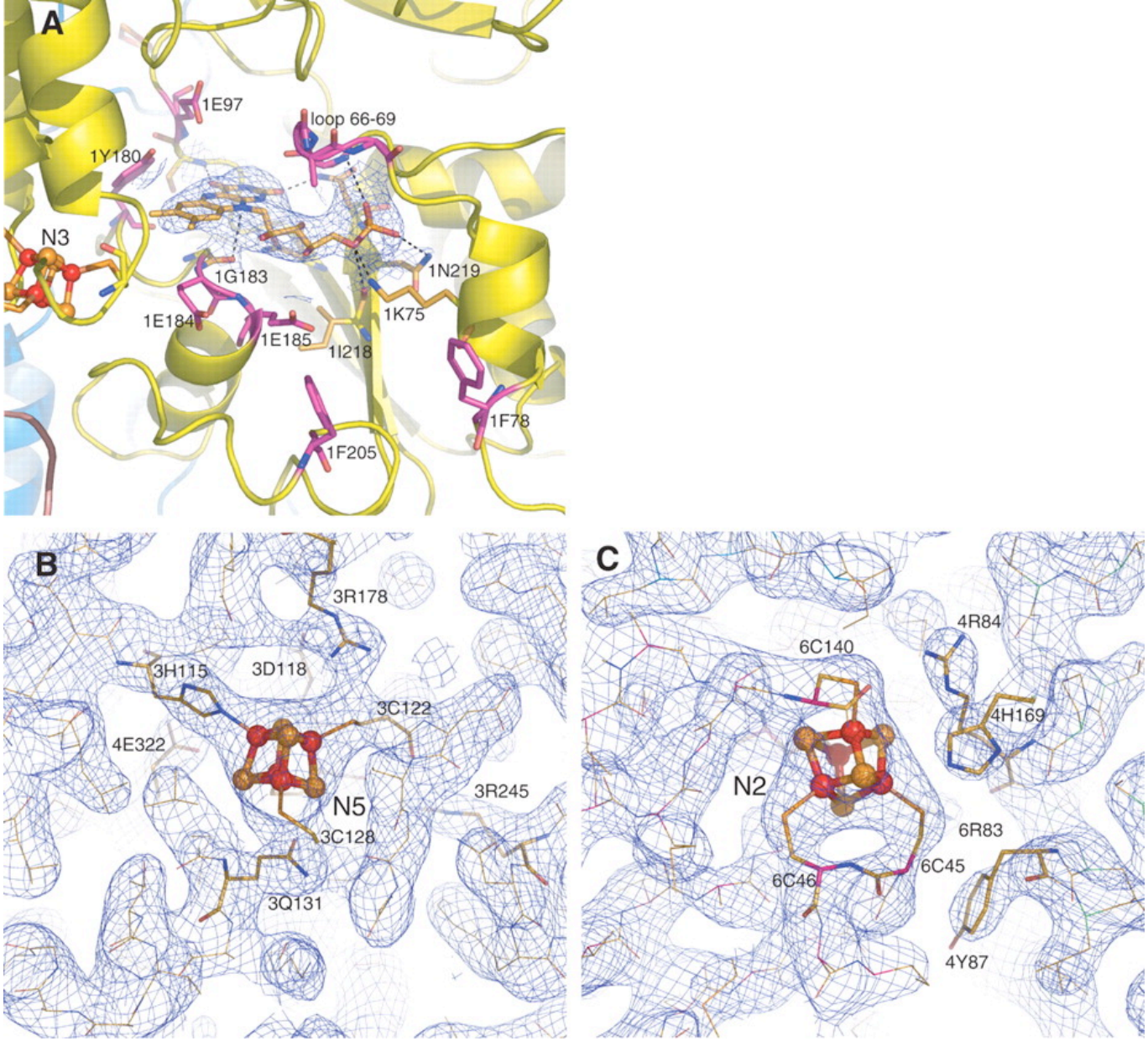

Fig. 3. The environments of the FMN-binding site and of selected Fe-S clusters. (**A**) The binding site for FMN and NADH, viewed from the solvent-exposed side. Residues involved in FMN binding are shown in stick representation with carbon in yellow and hydrogen bonds as dotted lines. Residues likely to be involved in NADH binding are shown in stick representation, with carbon in magenta. Prefixes to residue names indicate the subunit number. Cluster N3 is visible to the left. Subunits are colored as in Fig. 1. A $_{A}$-weighted $2F_{obs} - F_{calc}$ map contoured at 1 is shown around the FMN. (**B**) Cluster N5 and (**C**) cluster N2. Cluster ligands and polar residues nearby are shown. The backbones of subunits are colored as in Fig. 1. Electron density is from a $_{A}$-weighted $2F_{obs} - F_{calc}$ map contoured at 1. Clusters are shown as spheres of 0.3 van der Waals radius.

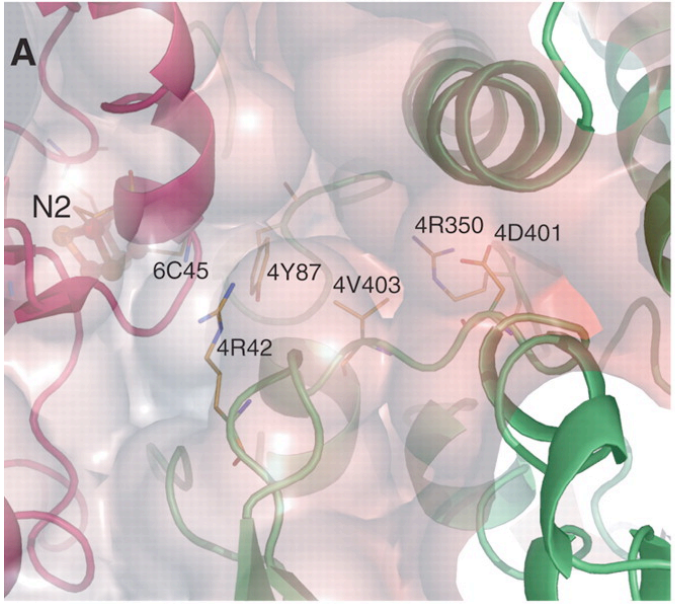

Fig. 4. Possible quinone- and iron-binding sites. The solvent-accessible surface area is shown, calculated with the APBS plug-in in PyMOL using a sphere of 1.4 Å radius as a probe. It is colored red for negative, white for neutral, and blue for positive surface charges. (**A**) Close-up of the quinone-binding site, viewed from the membrane space up toward the peripheral arm. Residues likely to interact with the quinone are shown. Prefixes before residue names indicate the subunit number. Subunits are colored as in Fig. 1. (**B**) Overview of the interface with the membrane domain in surface representation. The orientation is similar to that in (A). The quinone-binding site is indicated by an arrow and Q. Helix H1 and subunit names are indicated for orientation. (**C**) A possible iron-binding and/or iron storage site. Histidines and other polar residues lining the cavity are shown.

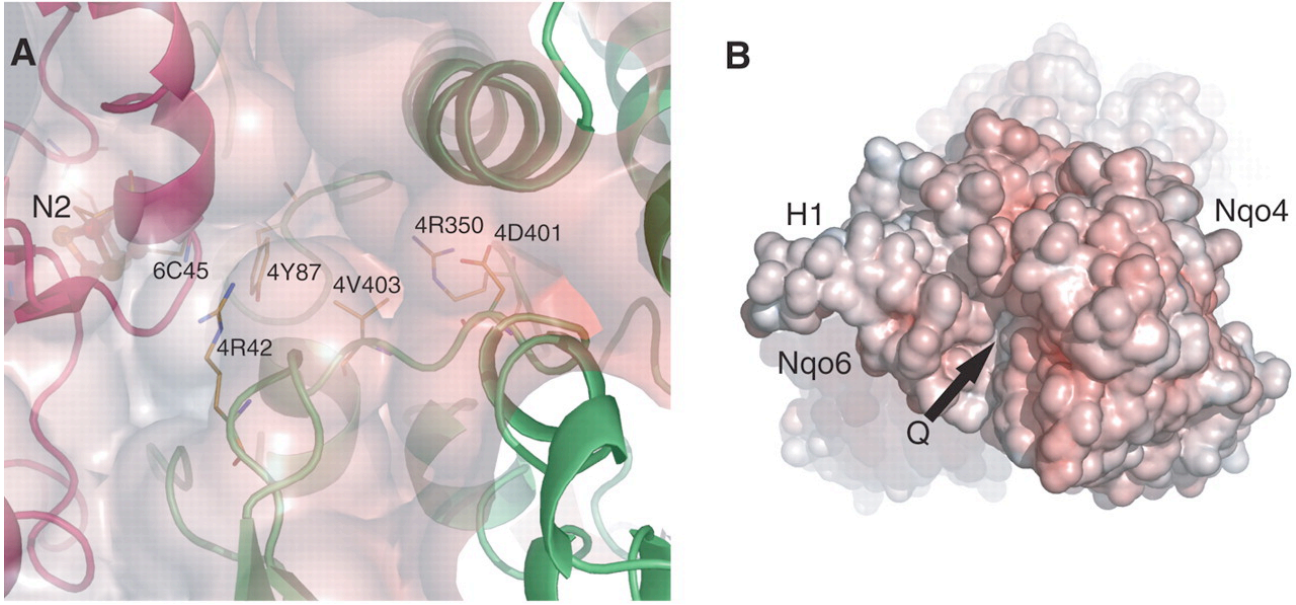

Fig. 4. Possible quinone- and iron-binding sites. The solvent-accessible surface area is shown, calculated with the APBS plug-in in PyMOL using a sphere of 1.4 Å radius as a probe. It is colored red for negative, white for neutral, and blue for positive surface charges. (**A**) Close-up of the quinone-binding site, viewed from the membrane space up toward the peripheral arm. Residues likely to interact with the quinone are shown. Prefixes before residue names indicate the subunit number. Subunits are colored as in Fig. 1. (**B**) Overview of the interface with the membrane domain in surface representation. The orientation is similar to that in (A). The quinone-binding site is indicated by an arrow and Q. Helix H1 and subunit names are indicated for orientation. (**C**) A possible iron-binding and/or iron storage site. Histidines and other polar residues lining the cavity are shown.

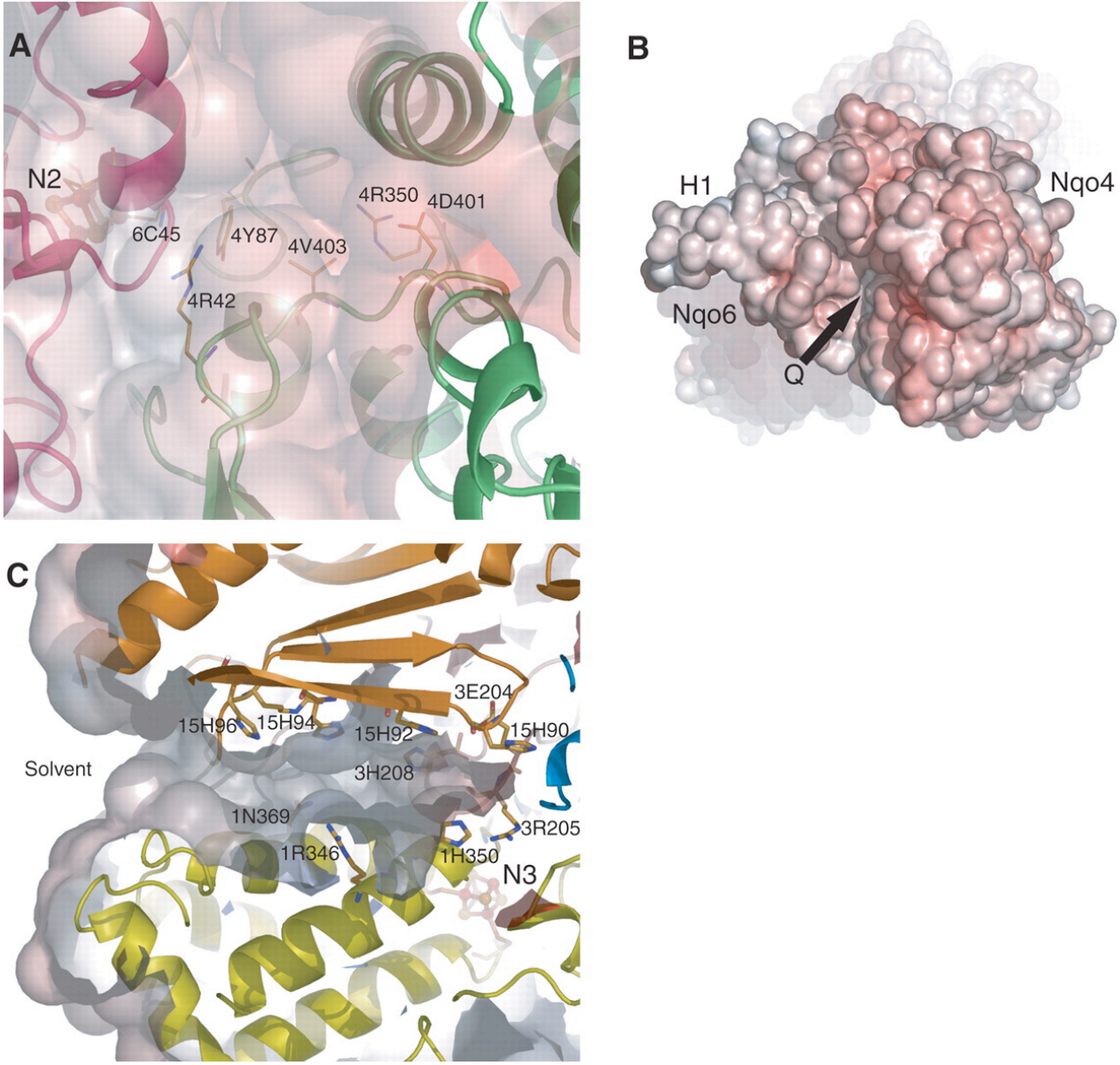

Fig. 4. Possible quinone- and iron-binding sites. The solvent-accessible surface area is shown, calculated with the APBS plug-in in PyMOL using a sphere of 1.4 Å radius as a probe. It is colored red for negative, white for neutral, and blue for positive surface charges. (**A**) Close-up of the quinone-binding site, viewed from the membrane space up toward the peripheral arm. Residues likely to interact with the quinone are shown. Prefixes before residue names indicate the subunit number. Subunits are colored as in Fig. 1. (**B**) Overview of the interface with the membrane domain in surface representation. The orientation is similar to that in (A). The quinone-binding site is indicated by an arrow and Q. Helix H1 and subunit names are indicated for orientation. (**C**) A possible iron-binding and/or iron storage site. Histidines and other polar residues lining the cavity are shown.

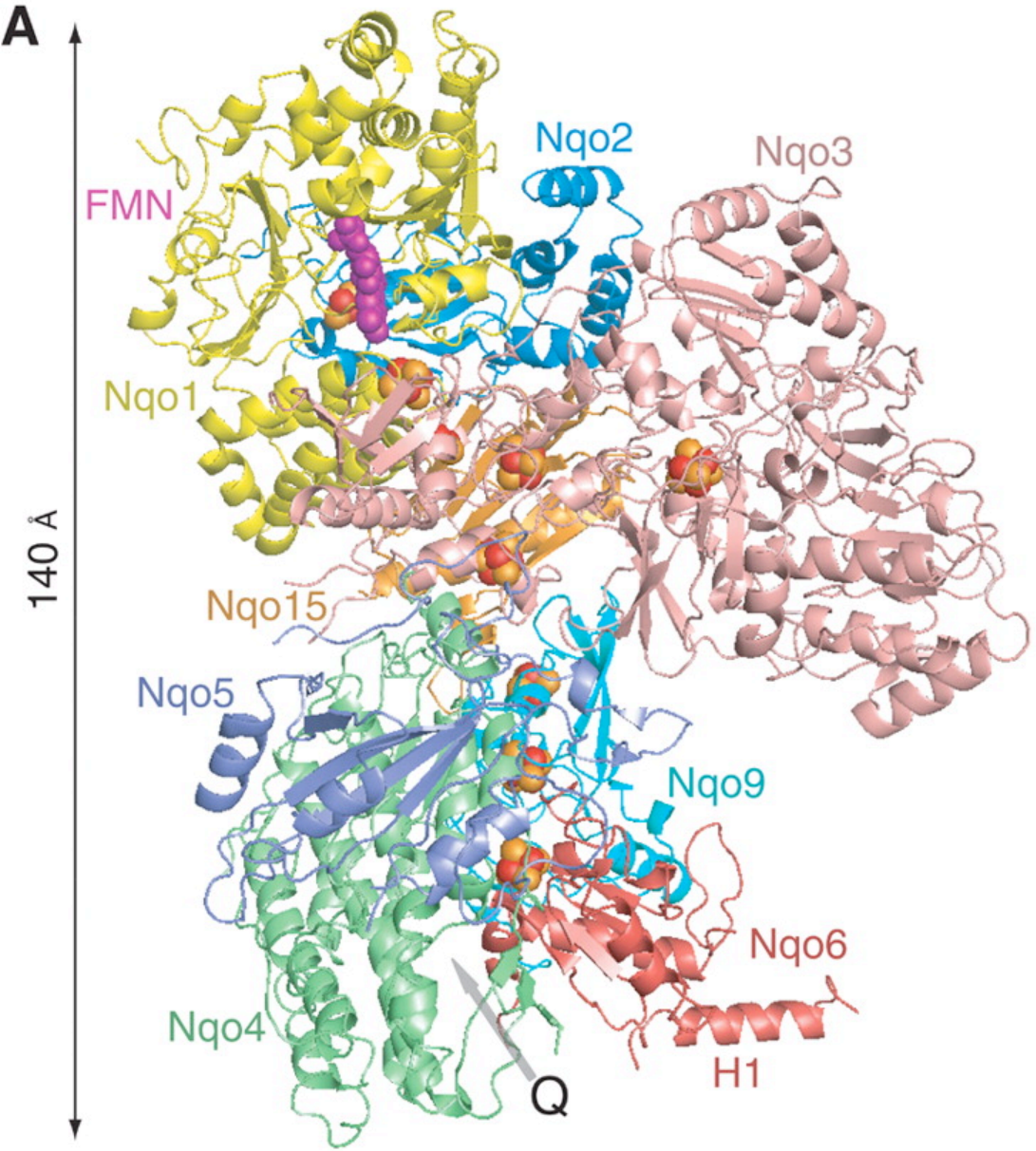
A
140 Å
FMN
Nqo2
Nqo3
Nqo1
Nqo15
Nqo5
Nqo9
Nqo6
Nqo4
H1
Q

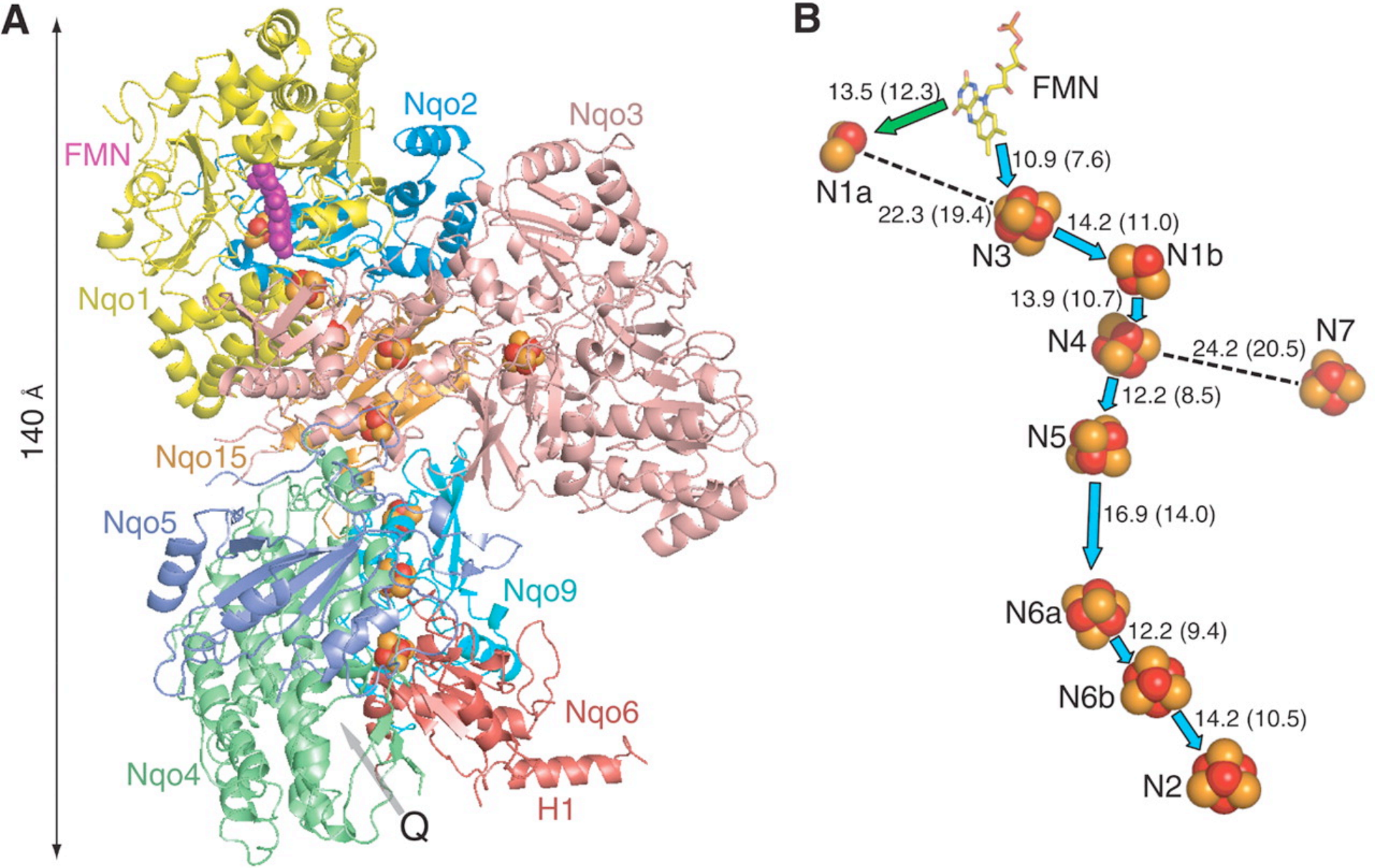
A
140 Å
FMN
Nqo2
Nqo3
Nqo1
Nqo15
Nqo5
Nqo9
Nqo6
Nqo4
H1
Q
B
FMN
13.5 (12.3)
N1a
10.9 (7.6)
22.3 (19.4)
N3
14.2 (11.0)
N1b
13.9 (10.7)
N4
24.2 (20.5)
N7
12.2 (8.5)
N5
16.9 (14.0)
N6a
12.2 (9.4)
N6b
14.2 (10.5)
N2

Hot topics http://www.scripps.edu/mem/biochem/CI/research.html

Topic 1: **Where are proton-translocating site(s) and quinone-binding site(s)?**It is generally believed that the energy coupling site(s) in complex I is located between Center N2 (the highest mid redox potential [4Fe-4S] cluster) and electron acceptor quinone. However, the location(s) has not been identified yet. In addition, there is no consensus about the number of coupling sites in complex I.

Hot topics http://www.scripps.edu/mem/biochem/CI/research.html

Topic 1: **Where are proton-translocating site(s) and quinone-binding site(s)?**It is generally believed that the energy coupling site(s) in complex I is located between Center N2 (the highest mid redox potential [4Fe-4S] cluster) and electron acceptor quinone. However, the location(s) has not been identified yet. In addition, there is no consensus about the number of coupling sites in complex I.

Topic 2: **Can Complex I pump not only protons but also sodium ions?** Recently, Steuber's group demonstrated that complex I in certain bacteria can work as a sodium pump. A question arises whether this feature is common to complex I of other sources.

Hot topics http://www.scripps.edu/mem/biochem/CI/research.html

Topic 1: **Where are proton-translocating site(s) and quinone-binding site(s)?**It is generally believed that the energy coupling site(s) in complex I is located between Center N2 (the highest mid redox potential [4Fe-4S] cluster) and electron acceptor quinone. However, the location(s) has not been identified yet. In addition, there is no consensus about the number of coupling sites in complex I.

Topic 2: **Can Complex I pump not only protons but also sodium ions?** Recently, Steuber's group demonstrated that complex I in certain bacteria can work as a sodium pump. A question arises whether this feature is common to complex I of other sources.

Topic 3: **Are accessory subunits in mitochondrial complex I really accessory?**Weiss'group and Walker's group reported that acyl carrier protein of the bacterial fatty acid synthesis system is a subunit of complex I. Hatefi's group and Schulte's group showed that the HP39k subunit binds NADPH. Papa's group reported that the IP18k subunit is phosphorylated and this phosphorylation is involved in regulation of complex I activity. Videira's group suggested involvement of some subunits in the assembly of *N. crassa* complex I. Recently, Scheffler's group demonstrated that the MWFE subunit is essential for complex I activity. These results raise a question as to whether "the accessory subunits" are really accessory.

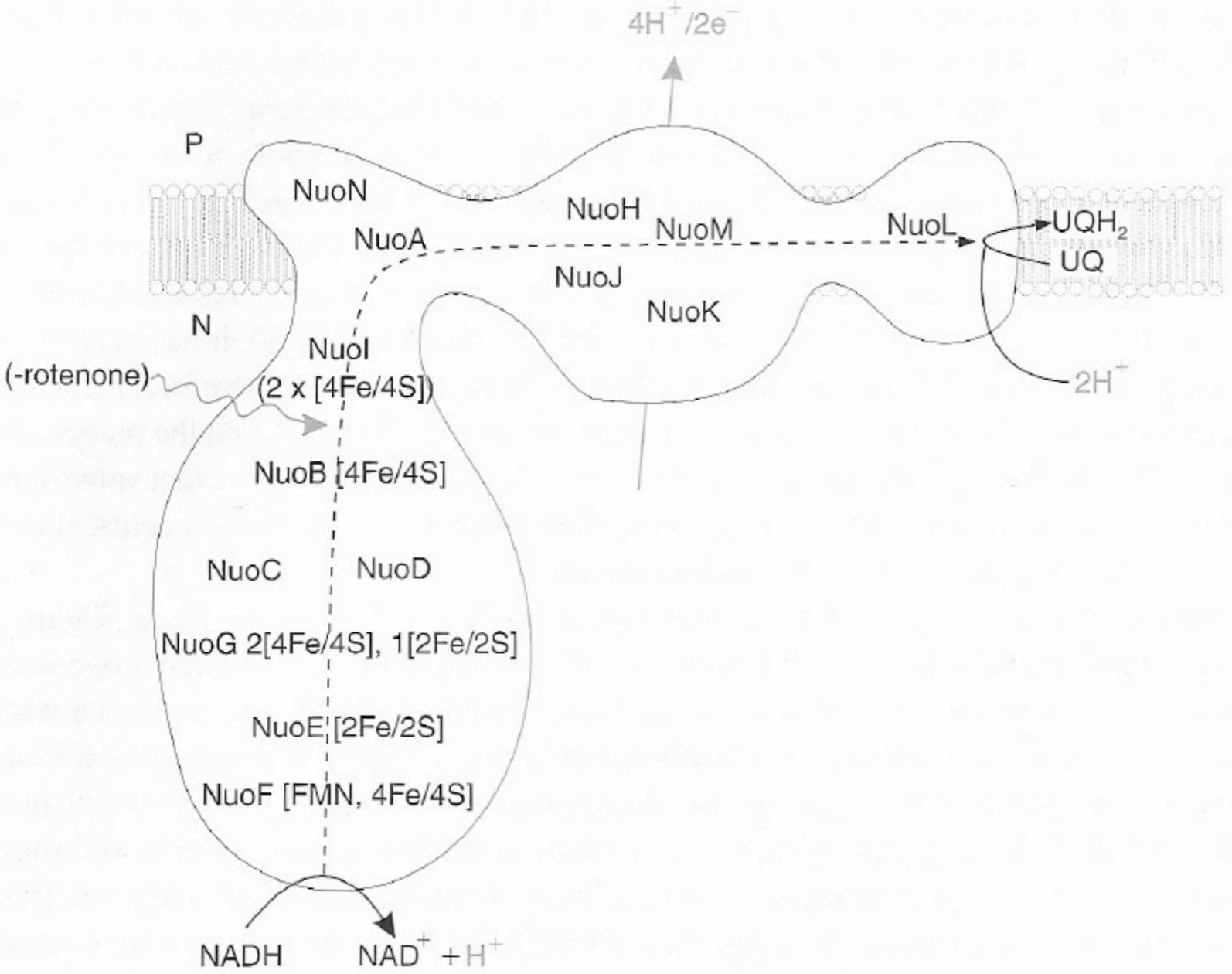

Figure 5.12 An outline structure for the mitochondrial (and bacterial) proton-translocating NADH–ubiquinone oxidoreductase (complex I).

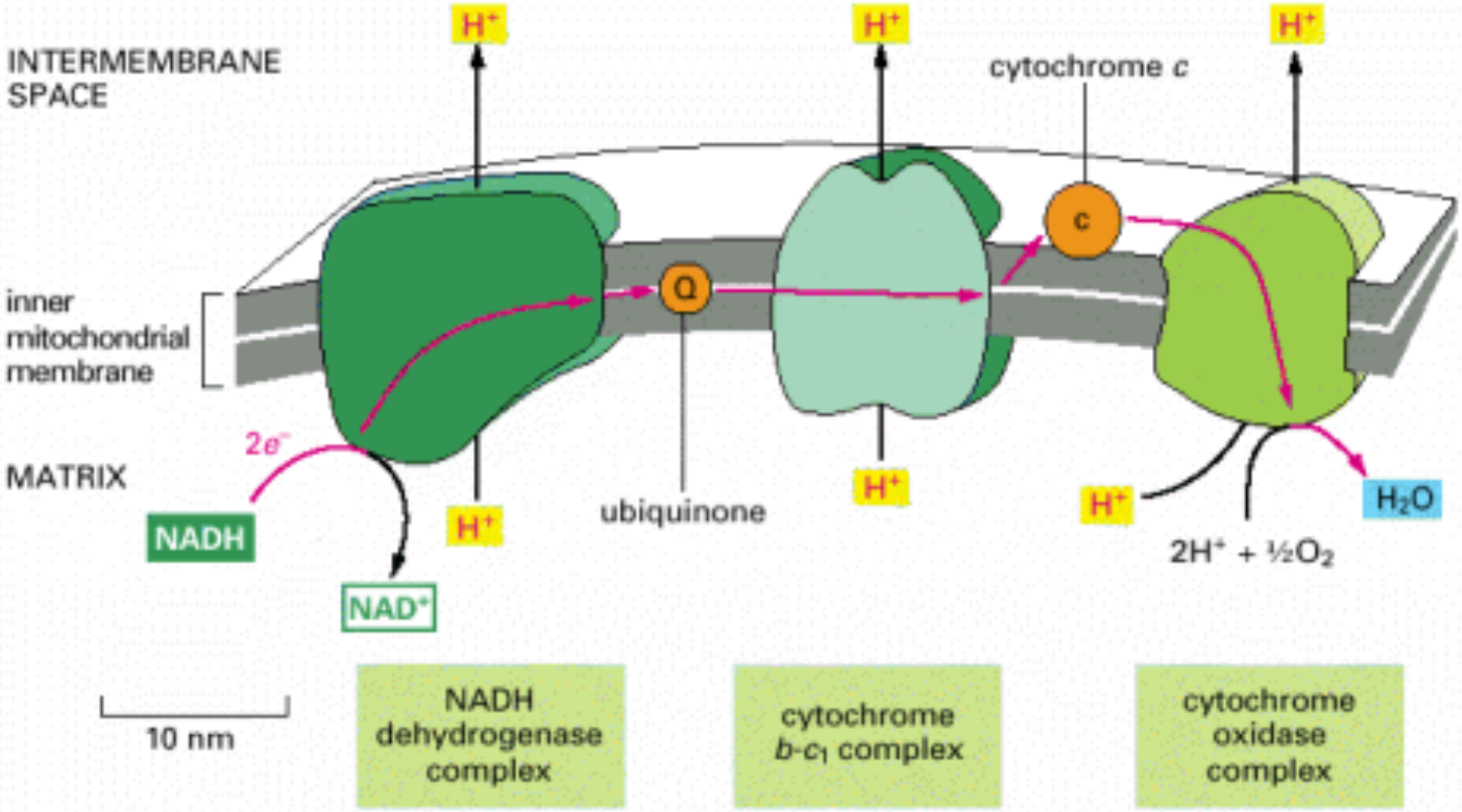

The Respiratory Chain Includes Three Large Enzyme Complexes Embedded in the Inner Membrane

Molecular Biology of the Cell Bruce Alberts, Alexander Johnson, Julian Lewis, Martin Raff, Keith Roberts, and Peter Walter. 2002

Next lecture

Complex I. Part 2. Complete structure, including the hydrophobic domain.

jfallen.org/lectures/

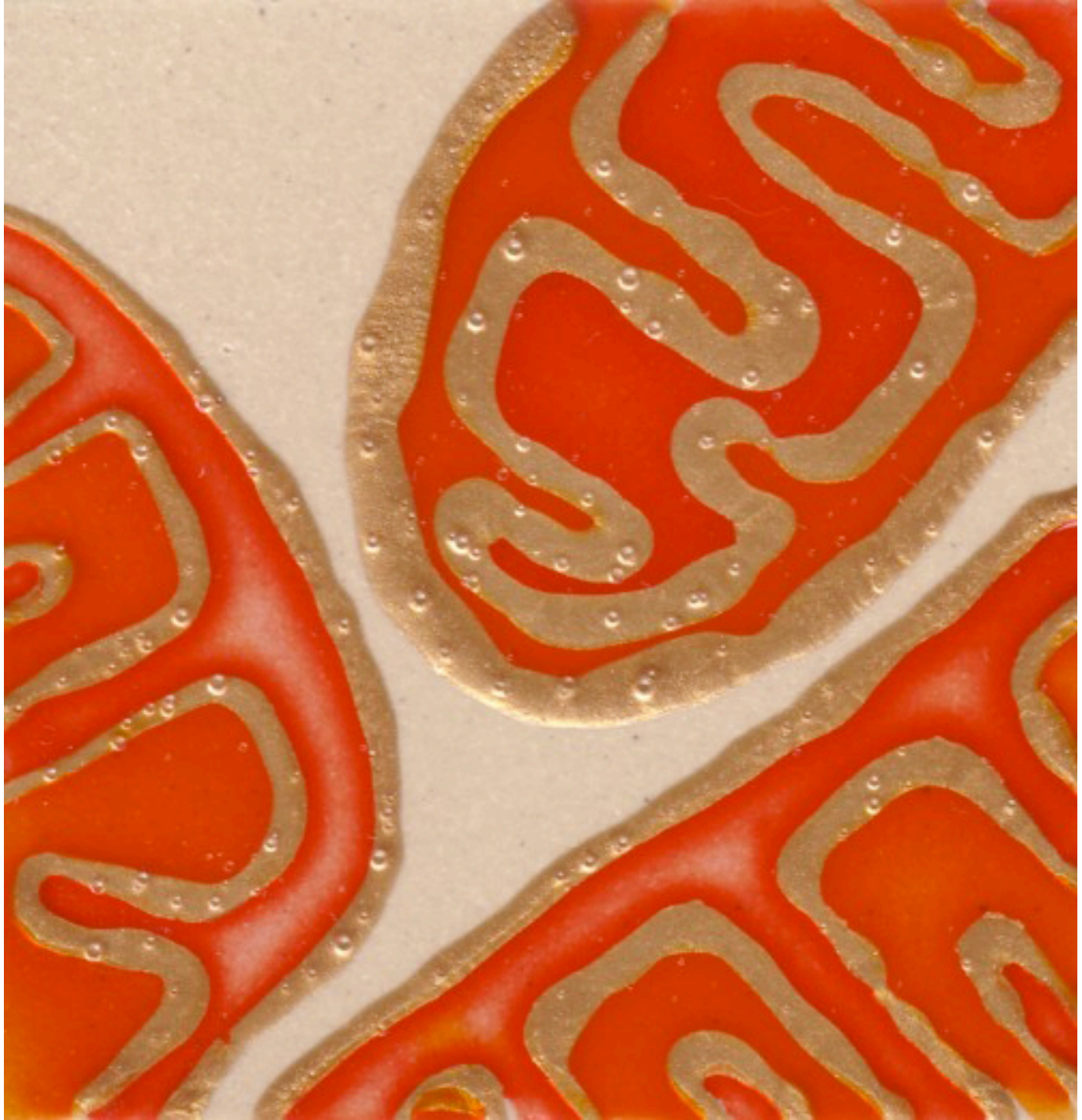


Thank you for listening


JVK
2004